



HAL
open science

A number-between-events control chart for monitoring nite horizon production processes

Arne Johannssen, Nataliya Chukhrova, Giovanni Celano, Philippe Castagliola

► To cite this version:

Arne Johannssen, Nataliya Chukhrova, Giovanni Celano, Philippe Castagliola. A number-between-events control chart for monitoring nite horizon production processes. *Quality and Reliability Engineering International*, 2022, 38 (4), pp.2110-2138. 10.1002/qre.3068 . hal-03661659

HAL Id: hal-03661659

<https://hal.science/hal-03661659v1>

Submitted on 7 May 2022

HAL is a multi-disciplinary open access archive for the deposit and dissemination of scientific research documents, whether they are published or not. The documents may come from teaching and research institutions in France or abroad, or from public or private research centers.

L'archive ouverte pluridisciplinaire **HAL**, est destinée au dépôt et à la diffusion de documents scientifiques de niveau recherche, publiés ou non, émanant des établissements d'enseignement et de recherche français ou étrangers, des laboratoires publics ou privés.

A number-between-events control chart for monitoring finite horizon production processes

Arne Johannssen*

Nataliya Chukhrova[†]

Giovanni Celano[‡]

Philippe Castagliola[§]

Abstract

In this paper, we present a number-between-events (NBE) control chart for monitoring the fraction nonconforming in finite horizon production (FHP) processes and related specific performance measures. When monitoring fractions nonconforming in FHP processes, the common binomial p -chart has two crucial limitations: the underlying distributional assumptions are violated when dealing with low-volume production and a scarce efficiency in the case of processes characterized by a low fraction nonconforming. Thus, an efficient monitoring of FHP processes requires the selection of the correct underlying statistical model: in this case, a distribution from the hypergeometric family of discrete statistical distributions. An efficient statistical monitoring of processes with low fractions nonconforming can be achieved by means of discrete time-between-events (TBE) control charts, which count the number of units up to the appearance of a fixed number of nonconforming units in the sample. Here, we present a discrete TBE-chart, denoted as NBE-chart, based on the negative hypergeometric distribution that meets numerous requirements of efficient monitoring of FHP processes. The proposed control chart can be conveniently used for both low-volume and mass production in processes with frequent changeovers.

Keywords: statistical process monitoring; control charts; number-between-events; finite horizon processes; fraction nonconforming; negative hypergeometric control chart

1 Introduction

Control charts are widely used in statistical process monitoring (SPM) for checking the stability of the fraction nonconforming or the counts of defects/nonconformities per unit vs. time. When implementing a control chart for monitoring the fraction nonconforming, it is worth remembering that an efficient on-line monitoring of processes characterized by low fractions nonconforming is a challenging task in many fields, such as modern manufacturing, service operations management, health care monitoring, public health surveillance, and education. In fact, the process yield is an important discriminating factor when a control chart should be selected to start process monitoring.

As the common binomial p control charts provide unsatisfactory results in monitoring processes with low fractions nonconforming p , several authors have presented and discussed control charts that take into account the time-between-events (TBE) to monitor the process. The TBE has been assumed by some authors as a continuous random variable corresponding to the time until the appearance of the r -th nonconforming unit in the sample (a so called *event*), with $r \in \mathbb{N}$. In this case, the exponential (case $r = 1$) or the Gamma distribution (case $r > 1$) is used for modeling the TBE (see, e.g., XIE et al.¹, CHENG et al.², KUMAR et al.³, SANUSI & MUKHERJEE⁴, ALEVIZAKOS & KOUKOUVINOS^{5,6}, SANUSI et

*University of Hamburg, Hamburg, Germany, arne.johannssen@uni-hamburg.de (corresponding author).

[†]University of Hamburg, Hamburg, Germany, nataliya.chukhrova@uni-hamburg.de.

[‡]University of Catania, Catania, Italy, giovanni.celano@unict.it.

[§]Université de Nantes & LS2N UMR CNRS 6004, Nantes, France, philippe.castagliola@univ-nantes.fr.

al.⁷, HU et al.^{8,9}), and the time T_r to the event is the variable plotted on the control chart. Conversely, other authors have considered the TBE as a discrete random variable by counting the *number* of units until the r -th nonconforming unit occurs in the sample: in this case, the geometric (case $r = 1$) or the negative binomial distribution (case $r > 1$) is utilized to model the TBE, and attribute control charts for nonconformities, generally known as cumulative count of conforming (CCC) charts, are proposed. There are some other common terms for these charts and their variants, such as CRL, RL1, CCC $_r$ or SCRL, and moreover, there are related charts such as CCS charts that are implemented to monitor the number of cumulative samples until a specified number of nonconforming products is detected (see ZHANG et al.¹⁰). For a comprehensive systematic review on TBE-charts, we refer to ALI et al.¹¹. For TBE-charts based on the geometric distribution see, e.g., CALVIN¹², GOH¹³, XIE & GOH¹⁴, NELSON¹⁵, CHAN et al.¹⁶, KURALMANI et al.¹⁷, RANJAN et al.¹⁸, ZHANG et al.¹⁹, NOOROSSANA et al.²⁰, ACOSTA-MEJIA²¹, CHIU & TSAI²², ZHANG et al.^{23,24}, GOLBAFIAN et al.²⁵, MORAIS²⁶, while TBE-charts based on the negative binomial distribution can be found, e.g., in OHTA et al.²⁷, CHAN et al.²⁸, DAS²⁹, DI BUCCHIANICO et al.³⁰, CHEN^{31,32}, ALBERS³³, ZHANG et al.³⁴.

The use of the geometric or the negative binomial distribution in attribute TBE-charts for nonconformities may be justified for monitoring continuous processes (e.g., mass production, comparable to *infinitely* large lot sizes), but they are inappropriate for constructing control charts to monitor *finite* lot sizes, like low-volume production of small batches of customized units.

In fact, in many real situations practitioners should cope with finite horizon production (FHP) processes, where the number of scheduled inspections m for quality control is set equal to a few tens and the lot size L is finite. FHP processes include the following production scenarios:

- high-volume production of L units (very large lot size) with frequent line changeovers and a slow inspection rate generating a *small* number m of inspections before the production ends: in this case, random sampling corresponds to a model of sampling *with* replacement;
- low-volume production of L customized units (small lot size) in a flexible manufacturing system releasing small batches of units and allowing for a *small* number m of scheduled inspections: in this case, random sampling corresponds to a model of sampling *without* replacement.

Whichever is the lot size L , monitoring of FHP processes is a challenging issue for quality engineers for the following reasons (see also CELANO & CASTAGLIOLA³⁵):

- When a process with FHP is run, the number of scheduled inspections is small, being it often fixed to a few tens. Process monitoring should be immediately started after the machine set-up and with no time to carry out a retrospective Phase I study on a preliminary set of samples. For this reason, a deviation-from-nominal value approach (also called a *standard-given* approach) should be considered to run the control chart when a target value can be specified by the practitioner. With standards given, the goal of FHP process monitoring is to check if it runs close to the nominal (target) value from the beginning to the end of the production run. Thus, to perform statistical process monitoring in a FHP process by means of an attribute control chart based on nonconformities, the definition of a target value p_0 for the fraction nonconforming is required to practitioners. Next, the control chart should be used to decide if the process is shifting from the target value p_0 . That is, by running the control chart in a FHP process, the quality practitioner is interested in checking if the fraction nonconforming remains "on-target" or is "out-of-target" during the production run.

- The inspection lot size $N = \lceil \frac{L}{m} \rceil$ can be so small that a finite population effect should be considered for the definition of a sound statistical model at the basis of the implementation of a control chart for monitoring the fraction nonconforming.
- The control chart's performance should be measured by metrics accounting for the small number of scheduled inspections during the production run. In fact, long run metrics of performance like the average run length (ARL) are unsuitable for a FHP process.

Since the development of control charts for monitoring FHP processes, the attention of researchers has mainly been focused on variable control charts. For instance, NENES et al.³⁶ and NENES et al.³⁷ presented a Markov chain approach for the exact computation of the statistical performance of the variable sampling interval control chart and of any fully adaptive Shewhart control chart in processes with an unknown but finite number of inspections, respectively. CELANO et al.^{38,39} and CELANO & CASTAGLIOLA⁴⁰ proposed the implementation of the Shewhart and EWMA sign control chart for both mass and low-volume production, respectively. CELANO et al.⁴¹ compared the performance of several control charts jointly monitoring both location and scale for observations with a location-scale distribution for a FHP process. CELANO & CASTAGLIOLA⁴² discussed the implementation of a control chart for on-line monitoring of extreme values of geometric profiles in FHP processes. Additionally, CELANO & CHAKRABORTI⁴³ investigated the issues related to the implementation of Mann-Whitney control charts for monitoring the location in FHP processes.

In this scenario, a correct investigation of attribute control charts for monitoring the fraction nonconforming in a FHP process calls for the definition of a sound statistical theory allowing for the flexibility of monitoring both low-volume and high-volume production. Recently, p and np charts based on the hypergeometric distribution have been proposed to account for the lot size effect in periodical processes, but without taking into account the characteristics of FHP processes, see CHUKHROVA & JOHANNSEN^{44,45} and JOHANNSEN et al.⁴⁶. However, efficient monitoring of FHP processes requires an adequate embedding of their characteristics in the modeling and thus a specific control chart design and different performance measures than for monitoring processes that do not have a finite horizon. As a matter of fact, the negative hypergeometric distribution turns out to be a promising statistical model to run an attribute control chart in a FHP process, when the value of p is too small to have an efficient implementation of the p control chart.

Therefore, we present in this paper a negative hypergeometric control chart that has the best prerequisites for an efficient monitoring of finite horizon processes. This chart belongs to the family of *discrete* TBE control charts. However, to avoid confusion with the term "time", we denote it as a "number-between-events" (NBE) control chart, following a similar notation as introduced by BENNEYAN⁴⁷. For this reason, we also refer to geometric and negative binomial charts as NBE-charts.

The paper is structured as follows. Section 2 briefly introduces the properties of the negative hypergeometric distribution and its limiting case for a very large population size. In Section 3, we present the negative hypergeometric NBE-chart for monitoring FHP processes and analyze its properties analytically. Afterward, in Section 4 we discuss performance measures and design of the negative hypergeometric NBE-chart in a FHP process. In Section 5, we perform a comprehensive on-target and out-of-target performance study. Section 6 illustrates a practical application of the proposed NBE-chart. Conclusions and future research directions in Section 7 complete the paper.

2 The negative hypergeometric distribution and its properties

2.1 The negative hypergeometric distribution

Let us consider a finite population of size N containing M objects classified as *successes*. The number y of draws without replacement from the population until r successes are counted is a random variable Y which has a negative hypergeometric distribution, i.e., $Y \sim \text{NH}(N, M, r)$ where $y, N, M, r \in \mathbb{N}^*$, $r \leq M \leq N$, $r \leq y \leq N$. By definition, Y is defined on $\{r, r+1, \dots, N-M+r\}$ and its probability mass function (p.m.f.) is given by:

$$\mathbb{P}_{\text{NH}}(Y = y) = \frac{\binom{y-1}{r-1} \binom{N-y}{M-r}}{\binom{N}{M}} \quad (2.1)$$

The mean and variance of Y are defined as

$$\mathbb{E}_{\text{NH}}[Y] = \frac{r(N+1)}{M+1} \quad \text{and} \quad \text{Var}_{\text{NH}}(Y) = \frac{r(N+1)(N-M)(M+1-r)}{(M+1)^2(M+2)}, \quad (2.2)$$

respectively. The cumulative distribution function (c.d.f.) of Y is given by:

$$F_{\text{NH}}(y) = \mathbb{P}_{\text{NH}}(Y \leq y) = \sum_{k=r}^y \frac{\binom{k-1}{r-1} \binom{N-k}{M-r}}{\binom{N}{M}} \quad (2.3)$$

For $N \rightarrow \infty$, (2.1) converges to the p.m.f. of a negative binomial-distributed random variable $Y \sim \text{NB}(r, p)$:

$$\mathbb{P}_{\text{NB}}(Y = y) = \binom{y-1}{r-1} p^r (1-p)^{y-r}, \quad (2.4)$$

where Y is defined on $\{r, r+1, \dots\}$ and $p = \frac{M}{N} \in (0, 1]$. Note that there are other definitions of the negative binomial distribution, see, e.g., JOHNSON et al.⁴⁸. Due to the result (2.4), the moments $\mathbb{E}_{\text{NH}}[Y]$ and $\text{Var}_{\text{NH}}(Y)$ converge to

$$\mathbb{E}_{\text{NB}}[Y] = \frac{r}{p} \quad \text{and} \quad \text{Var}_{\text{NB}}(Y) = \frac{r(1-p)}{p^2},$$

and the c.d.f. of Y is given by

$$F_{\text{NB}}(y) = \mathbb{P}_{\text{NB}}(Y \leq y) = \sum_{k=r}^y \binom{k-1}{r-1} p^r (1-p)^{k-r}. \quad (2.5)$$

2.2 Some properties of the negative hypergeometric distribution

In this paper, some properties of the negative hypergeometric distribution are required to implement the proposed NBE control chart. Therefore, we briefly discuss them in this Section.

First of all, we compare $\mathbb{E}_{\text{NH}}[Y]$ to $\mathbb{E}_{\text{NB}}[Y]$ and $\text{Var}_{\text{NH}}(Y)$ to $\text{Var}_{\text{NB}}(Y)$. Considering $\mathbb{E}[Y]$, it holds:

$$\mathbb{E}_{\text{NH}}[Y] = \frac{r(N+1)}{M+1} < \frac{rN}{M} = \frac{r}{p} = \mathbb{E}_{\text{NB}}[Y] \quad \text{for } M < N.$$

Thus, we have $\mathbb{E}_{\text{NH}}[Y] < \mathbb{E}_{\text{NB}}[Y]$ and $\mathbb{E}_{\text{NH}}[Y] = \mathbb{E}_{\text{NB}}[Y] = r$ only holds when $M = N$. With regard to

$\text{Var}(Y)$ it holds:

$$\text{Var}_{\text{NH}}(Y) = \underbrace{\frac{r(N+1)}{M+1}}_{< \frac{r}{p}} \cdot \underbrace{\frac{N-M}{M+1}}_{< \frac{N-M}{M}} \cdot \underbrace{\frac{M+1-r}{M+2}}_{< 1} < \underbrace{\frac{r}{p} \cdot \frac{1-p}{p}}_{= \frac{N-M}{M}} = \text{Var}_{\text{NB}}(Y) \quad \text{for } M < N.$$

Thus, we have $\text{Var}_{\text{NH}}(Y) < \text{Var}_{\text{NB}}(Y)$ and $\text{Var}_{\text{NH}}(Y) = \text{Var}_{\text{NB}}(Y) = 0$ only holds when $M = N$.

Since the c.d.f. of the negative hypergeometric distribution is rarely included in common software, such as MATLAB and MS Excel, we provide a simple relationship between the c.d.f. shown in (2.3) and the c.d.f. of a hypergeometric-distributed random variable $X \sim \text{H}(N, M, y)$ (see, e.g., JOHNSON et al. ⁴⁸):

$$F_{\text{NH}}(y) = 1 - \mathbb{P}_{\text{H}}(X \leq r-1) = 1 - \sum_{x=0}^{r-1} \frac{\binom{M}{x} \binom{N-M}{y-x}}{\binom{N}{y}} \quad (2.6)$$

Considering the negative binomial distribution, there is an analogous relationship between (2.5) and the c.d.f. of a binomial-distributed random variable $X \sim \text{B}(y, p)$ (see, e.g., CHEN ³¹):

$$F_{\text{NB}}(y) = 1 - \mathbb{P}_{\text{B}}(X \leq r-1) = 1 - \sum_{x=0}^{r-1} \binom{y}{x} p^x (1-p)^{y-x} \quad (2.7)$$

3 Statistical process monitoring of fraction nonconforming in a FHP process

We consider a lot production of $L \in \mathbb{N}^*$ units during a finite production horizon H . Quality monitoring should be performed by scheduling a finite number $m \in \mathbb{N}^*$ of inspections during the production. At each inspection a set of $N = \lceil \frac{L}{m} \rceil \in \mathbb{N}^*$ units, from now on denoted as the *inspection lot*, is available for monitoring: these are the N units of the production lot released by the manufacturing system before the first inspection ($m \geq 1$) and, if applicable, between two consecutive inspections ($m \geq 2$). The quality practitioner is interested in checking the occurrence of shifts in the fraction nonconforming p during the production run by monitoring each inspection lot. A target value p_0 is fixed by the quality practitioner according to the order requirements agreed with the customer or the quality characteristics' specifications settled by the organization.

3.1 The negative hypergeometric NBE-chart for lot production

If a small lot of L units is produced, quality monitoring should be performed by a control chart suitable to cope with finite lot sizes. Here, we consider the negative hypergeometric NBE-chart to monitor the fraction nonconforming. Let Y_j , $j = 1, \dots, m$, be the number of units sampled *without* replacement at the j -th inspection from the j -th inspection lot of size N_j until the r -th nonconforming unit occurs. If the count of nonconforming units within the inspection lot j is less than r , then $Y_j = N_j$, for $j = 1, \dots, m$. Being the inspections scheduled at fixed sampling intervals, under the assumption of a fixed production rate it holds $N_1 = N_2 = \dots = N_m = N$. Thus, we denote N as the fixed inspection lot size. At each inspection j , $j = 1, \dots, m$, the minimum and maximum number of units to be inspected is equal to r and N , respectively, i.e., $r \leq Y_j \leq N$. Hence, Y_1, \dots, Y_m are i.i.d. outcomes of a negative hypergeometric-distributed random variable $Y \sim \text{NH}(N, M, r)$ with p.m.f. (2.1), c.d.f. (2.3) and first moments given by (2.2). The fraction nonconforming $p = \frac{M}{N}$ is defined with respect to the inspection lot size N ; M is the expected number of nonconforming units within each inspection lot, given p . Therefore, if the process

runs on-target (out-of-target), then $p = p_0$ ($p = p_1$) and $M = Np_0$ ($M = Np_1$). The target value of $\mathbb{E}_{\text{NH}}[Y]$ is equal to:

$$Y_0 = \frac{r(N+1)}{1+Np_0} \quad (3.1)$$

Given the target value Y_0 , the Shewhart-type negative hypergeometric NBE-chart has center line CL_{NH} , upper and lower control limit UCL_{NH} and LCL_{NH} defined as:

$$\begin{aligned} \text{UCL}_{\text{NH}} &= Y_0 + d_u \sqrt{Y_0 \left(\frac{Y_0}{r} - 1 \right) \frac{rN_1 - Y_0}{rN_1 + Y_0}} \\ \text{CL}_{\text{NH}} &= Y_0 \\ \text{LCL}_{\text{NH}} &= \max \left\{ 0, Y_0 - d_l \sqrt{Y_0 \left(\frac{Y_0}{r} - 1 \right) \frac{rN_1 - Y_0}{rN_1 + Y_0}} \right\} \end{aligned} \quad (3.2)$$

where $N_1 = N+1$, and the parameters $d_u \in \mathbb{R}_+$ and $d_l \in \mathbb{R}_+$ represent multiples of the standard deviation $\sqrt{Y_0 \left(\frac{Y_0}{r} - 1 \right) \frac{rN_1 - Y_0}{rN_1 + Y_0}}$ obtained to compute the width of control limits UCL_{NH} and LCL_{NH} , respectively. See Appendix A for a proof of (3.2).

The negative hypergeometric NBE-chart can be implemented for on-line monitoring on a lot of size L with inspection plan (m, r, N) only if $p_0 \geq \frac{r}{N} = \frac{r \cdot m}{L}$, with $N = \lceil \frac{L}{m} \rceil$. Therefore, the feasible number of scheduled inspections m is defined as $m \in \{1, \dots, \frac{p_0 \cdot L}{r}\}$ with $m \in \mathbb{N}^*$.

When the lot size L is very large (high-volume production in a FHP process) and m is specified such that N is large, the negative hypergeometric converges to the negative binomial statistical model. In this case, the control limits (LCL_{NH} , UCL_{NH}) and the center line CL_{NH} of the negative hypergeometric NBE control chart can be well approximated by the following formulas which are known as negative binomial NBE-chart:

$$\begin{aligned} \text{UCL}_{\text{NB}} &= Y_0 + d_u \sqrt{Y_0 \left(\frac{Y_0}{r} - 1 \right)} \\ \text{CL}_{\text{NB}} &= Y_0 \\ \text{LCL}_{\text{NB}} &= \max \left\{ 0, Y_0 - d_l \sqrt{Y_0 \left(\frac{Y_0}{r} - 1 \right)} \right\} \end{aligned} \quad (3.3)$$

where

$$Y_0 = \lim_{N \rightarrow \infty} \frac{r(N+1)}{1+Np_0} = \frac{r}{p_0}, \quad (3.4)$$

and the parameters $d_u \in \mathbb{R}_+$ and $d_l \in \mathbb{R}_+$ represent multiples of the standard deviation $\sqrt{Y_0 \left(\frac{Y_0}{r} - 1 \right)}$ obtained to compute the width of control limits UCL_{NB} and LCL_{NB} , respectively.

3.2 Statistical properties of the negative hypergeometric NBE-chart

The control limit interval $[\text{LCL}_{\text{NH}}, \text{UCL}_{\text{NH}}]$ of the negative hypergeometric NBE-chart is smaller than the control limit interval $[\text{LCL}_{\text{NB}}, \text{UCL}_{\text{NB}}]$ of the negative binomial NBE-chart when the population size is finite and $p < 1$. This follows directly from the fact that the control limits of the negative hypergeometric

and the negative binomial NBE-charts differ by the variance term and it holds $\text{Var}_{\text{NH}}(Y) < \text{Var}_{\text{NB}}(Y)$ for $M < N$ as well as $\text{Var}_{\text{NH}}(Y) = \text{Var}_{\text{NB}}(Y) = 0$ for $M = N$ (see Section 2.2).

Thus, for a given false alarm rate FAR_0 , the negative hypergeometric NBE-chart is more sensitive than the negative binomial NBE-chart to the same shift in the process quality level resulting in an increase of the process fraction nonconforming. This effect is due to sampling without replacement from a finite population having size N , since the number of units decreases with each inspection unit test.

Moreover, following the results discussed in Section 2.1, the center line and the control limits of both charts coincide as N gets larger values. In the case of a finite population size $\text{CL}_{\text{NH}} < \text{CL}_{\text{NB}}$ holds.

In the following we investigate analytically the impact of r , N , p_0 on the center line and the control limits of the negative binomial and negative hypergeometric NBE-chart, using (3.2) and (3.3) under consideration of (3.1) and (3.4), respectively.

- Impact of r : The larger is r (with $r \leq M$, $M, r \in \mathbb{N}^*$), the larger is the center line and the wider is the in-control interval of both charts.
- Impact of N : While the center line and the control limits of the negative binomial NBE-chart are not affected by N , conversely the center line increases and the in-control interval widens as N increases in the negative hypergeometric case. As shown above, for $N \rightarrow \infty$ the center line and the in-control interval of the negative hypergeometric NBE-chart converge to the center line and the in-control interval of the corresponding negative binomial NBE-chart, respectively.
- Impact of p_0 : Fixing a smaller value for p_0 increases the center line and the width of the in-control interval for both NBE-charts.

4 Performance measures and design of the NBE-chart in a FHP process

4.1 Power function of NBE-charts

The power function (PF) of an NBE-chart represents the probability function of rejecting the null hypothesis of statistical control ($H_0 : p = p_0$) depending on p . Thus, PF stands for the probability of a signal at each test inspection, given by

$$\text{PF} = \mathbb{P}(Y_j > \text{UCL}) + \mathbb{P}(Y_j < \text{LCL}) = 1 - \mathbb{P}(Y_j \leq \dot{U}) + \mathbb{P}(Y_j \leq \dot{L}) \quad (4.1)$$

with discretized control limits $\dot{U} = \max\{U \in \mathbb{N}^* | U \leq \text{UCL}\}$, $\dot{L} = \max\{L \in \mathbb{N} | L < \text{LCL}\}$. For $p = p_0$, PF stands for incorrect rejection of H_0 , i.e., the probability of the type I error $\alpha^* = \text{PF}_{p=p_0}$, while for $p = p_1$, with $p_1 \neq p_0$, PF implies correct rejection of H_0 . The probability of the type II error is given by $\beta^* = 1 - \text{PF}_{p=p_1}$. Note that these errors are indirect costs that characterize a control chart (see, e.g., PANAGIOTIDOU & TAGARAS⁴⁹).

Considering the negative hypergeometric and the negative binomial NBE-chart (that is, taking (2.3) and

(2.5)), respectively, (4.1) becomes:

$$PF_{NH} = 1 - \left(\sum_{k=r}^{\dot{U}} \frac{\binom{k-1}{r-1} \binom{N-k}{M-r}}{\binom{N}{M}} - \sum_{k=r}^{\dot{L}} \frac{\binom{k-1}{r-1} \binom{N-k}{M-r}}{\binom{N}{M}} \right) \quad (4.2)$$

$$PF_{NB} = 1 - \left(\sum_{k=r}^{\dot{U}} \binom{k-1}{r-1} p^r (1-p)^{k-r} - \sum_{k=r}^{\dot{L}} \binom{k-1}{r-1} p^r (1-p)^{k-r} \right) \quad (4.3)$$

By considering equations (2.6) and (2.7), we can simplify (4.2) and (4.3) as follows:

$$PF_{NH} = 1 - \left(\sum_{x=0}^{r-1} \frac{\binom{M}{x} \binom{N-M}{\dot{L}-x}}{\binom{N}{\dot{L}}} - \sum_{x=0}^{r-1} \frac{\binom{M}{x} \binom{N-M}{\dot{U}-x}}{\binom{N}{\dot{U}}} \right) \quad (4.4)$$

$$PF_{NB} = 1 - \left(\sum_{x=0}^{r-1} \binom{\dot{L}}{x} p^x (1-p)^{\dot{L}-x} - \sum_{x=0}^{r-1} \binom{\dot{U}}{x} p^x (1-p)^{\dot{U}-x} \right) \quad (4.5)$$

4.2 Performance measures of the negative hypergeometric NBE-chart in a FHP process

Since long run measures of performance like the ARL are unsuitable for a FHP process with a finite number m of inspections ($j = 1, \dots, m$), the performance of the negative hypergeometric NBE-chart should be measured by metrics accounting for the small number of scheduled inspections during the production run.

The on-target performance should be estimated by means of the false alarm rate (FAR) at each inspection $j = 1, \dots, m$ and the false alarm probability (FAP) during the production run (the overall probability of the type I error, i.e., the probability for at least one false alarm from m samples). To start on-line monitoring of FHP processes, the quality practitioner is interested to fix the nominal false alarm rate FAR_0 at a small value (i.e., $p_0^r \leq FAR_0 \leq 0.1$ due to a reasonable restriction of LCL given by $LCL_{\min} = r + 1$), if necessary and possible under the constraint of a reasonable fixation or minimization of the resulting FAP (see also Section 5.1). While FAR ($\alpha^* = PF_{p=p_0}$) is given by (4.4), FAP is defined as follows:

$$FAP = 1 - (1 - PF_{p=p_0})^m = 1 - (1 - \alpha^*)^m$$

The out-of-target performance of the proposed chart can be measured by the probability of a signal *at* each scheduled inspection after the occurrence of an assignable cause (SP) and the probability of a signal *by* the end of the production run (RSP) (see CELANO & CASTAGLIOLA^{35,40}). In particular, a signal triggered by the control chart warns practitioners about looking for the presence of an assignable cause and segregating the production lot, if needed. Both the out-of-target performance measures, SP and RSP, depend on the shift size δ of the process location, defined via $p_1 = p_0 + \delta$, and the position of the process change-point τ with respect to the scheduled end of the production horizon. In fact, for a given shift size δ , the closer is the change-point to the end of the production run, the lower is the probability of detecting the process shift (a true alarm) by the end of the run (see CELANO & CHAKRABORTI⁴³). While SP at the j -th inspection, $j = s, s + 1, \dots, m$, is dependent on the probability of the type II error,

$$SP_j = (1 - PF_{p=p_1})^{j-s} PF_{p=p_1} = (\beta^*)^{j-s} (1 - \beta^*),$$

RSP also depends on the number m of scheduled inspections:

$$\text{RSP} = 1 - (1 - \text{PF}_{p=p_1})^{m-s+1} = 1 - (\beta^*)^{m-s+1},$$

where $s = \lceil \frac{\tau \cdot m}{H} \rceil$ is the index identifying the first inspection scheduled immediately after the process change-point τ (hours), given a production horizon H (hours). The ceiling function $\lceil x \rceil$ maps x to the least integer greater than or equal to x . For example, if the process change-point occurs after $\tau = 3.5$ hours in a production run having a horizon of $H = 10$ hours and $m = 10$ scheduled inspections, then the first inspection with the shifted process is $s = \lceil 3.5 \rceil = 4$.

4.3 Design of NBE-charts

4.3.1 Computation of d_l and d_u

Commonly, the parameters d_l and d_u for the construction of Shewhart-type control limits are determined by using normal quantiles. That is, under the assumption of an appropriate normal approximation to the underlying distribution, e.g., the binomial distribution in the framework of p - and np -charts. Moreover, it is sometimes common practice to use normal quantiles also for NBE-charts based on geometric or negative binomial distribution (see, e.g., BENNEYAN^{47, 50}). The motivation behind this approach for computing the control limits is providing practitioners with a procedure as easy to implement as the traditional Shewhart-type $d\sigma$ control limits.

However, the normal approximation can lead to a too large error in the computation of the statistical measures for the NBE control chart (especially for small values of p_0 in combination with a small value of N). Therefore, in this paper we suggest to determine the parameters d_l and d_u via the c.d.f. of the exact underlying distribution. In addition, considering one-sided NBE-charts with only LCL is reasonable when practitioners are primarily interested in detecting increases of the process fraction nonconforming ($p_1 > p_0$). Then, UCL should not be considered as threshold for an alarm but rather as a criterion to stop sampling, if $Y_j > \text{UCL}$.

In general, the parameters d_l and d_u can only be calculated numerically. Thus, there is the need for a numerical solution regarding d_l and d_u . This solution can be obtained by running an iterative procedure using the cumulative (negative) hypergeometric distribution (see (2.6)). There is only one case where a closed formula exists for the computation of d_l , d_u : let us consider $r = 1$, $N \rightarrow \infty$ and a one-sided chart with LCL (that is, $\hat{U} \rightarrow \infty$). Setting (4.5) lower-equal to FAR_0 then gives us:

$$1 - ((1 - p_0)^{\hat{L}} - \underbrace{(1 - p)^{\hat{U}}}_{\rightarrow 0}) \leq \text{FAR}_0 \quad (4.6)$$

Using $\hat{L} = \lceil \text{LCL}_{\text{NB}} \rceil - 1$ with $\lceil \text{LCL}_{\text{NB}} \rceil = \lceil \text{CL}_{\text{NB}} - d_l \sqrt{\text{Var}_{\text{NB}}} \rceil$ and rearranging (4.6) for d_l , we obtain an inequality regarding d_l as follows:

$$-\frac{\ln((1 - \text{FAR}_0)(1 - p_0)) - \text{CL}_{\text{NB}} \ln(1 - p_0)}{\ln(1 - p_0) \sqrt{\text{Var}_{\text{NB}}}} \leq d_l \leq -\frac{\ln(1 - \text{FAR}_0) - \text{CL}_{\text{NB}} \ln(1 - p_0)}{\ln(1 - p_0) \sqrt{\text{Var}_{\text{NB}}}} \quad (4.7)$$

Since a larger value of d_l leads to a lower value of FAR_{NB} , and thus to the fulfillment of the constraint regarding FAR_0 , the right-hand side of (4.7) should be used to calculate d_l . In an analogous way, a closed formula for d_u can be derived, for instance when it is also important to detect examples for a good

practice (that is, $Y_j > \text{UCL}$).

4.3.2 Selection of m and r

Given the target proportion p_0 of nonconforming units as well as the total lot size L , the selection of the couple (m, r) with

$$m \in \left\{1, \dots, \frac{p_0 \cdot L}{r}\right\} \quad \text{and} \quad r \in \left\{1, \dots, \frac{p_0 \cdot L}{m}\right\}$$

could be done under the constraint $\text{FAR}_{\text{NH}} \leq \text{FAR}_0$, by maximizing the out-of-target performance measure RSP, as proposed for other control charts monitoring FHP processes (see, for example, CELANO & CHAKRABORTI⁴³). In this case, the couple $(m, r) = (1, Lp_0)$ would lead in general to the maximum RSP due to the steepest curve of the power function and thus the smallest possible type II error. However, the expected inspection effort is quite high for this (m, r) -combination and a shift in the process quality level can only be detected at the end of the production run. To account for this problem, we consider the average number ANU of released units after the occurrence of the assignable cause. In particular, based on a truncated geometric distribution, ANU is defined as

$$\text{ANU} = \left(\sum_{j=1}^{m-s+1} L \cdot \frac{j}{m} \cdot \text{PF}_{p=p_1} (1 - \text{PF}_{p=p_1})^{j-1} \right) + L \cdot \frac{m-s+1}{m} \cdot (1 - \text{PF}_{p=p_1})^{m-s+1}, \quad (4.8)$$

where the second term on the right side of (4.8) accounts for $\text{PF}_{p=p_1} < 1$ (and thus $\text{RSP} < 1$) and considers the contribution related to the probability of no signal by the end of the production run.

Specifying $m = 1$ and $s = 1$, we obtain $\text{ANU} = L$ for all $\text{PF}_{p=p_1} \in [0, 1]$, i.e., the maximum value of ANU. Since a practitioner desires the ANU to be as small as possible, the couples of design parameters (m, r) should be selected as to minimize ANU by considering $m > 1$ and finding the corresponding optimal value for r . Following this approach, the input parameters are $(L, p_0, p_1, \text{FAR}_0, s)$, the decision variables are (m, r) , the output values are $(N, M, d_i, \text{FAR}_{\text{NH}}, \text{RSP})$ and the objective function is ANU. Summarizing, the following design procedure has to be run:

1. Given the input parameters $(L, p_0, p_1, \text{FAR}_0, s)$

2. Select: $(m^*, r^*) = \arg \min_{(m, r)} (\text{ANU})$

s.t.

$$m \in \left\{1, \dots, \frac{p_0 \cdot L}{r}\right\}$$

$$r \in \left\{1, \dots, \frac{p_0 \cdot L}{m}\right\}$$

To determine the optimal values for m and r , we propose to apply a *brute-force search* as we deal in general with small values of p_0, L on the one hand and natural numbers m, r on the other hand. Thus, the set of all possible candidate solutions is limited by the number of combinations

$$\sum_{i=1}^{p_0 \cdot L} \frac{p_0 \cdot L}{i} \quad \text{with} \quad \frac{p_0 \cdot L}{i} \in \mathbb{N},$$

i.e., it is of a manageable size (very low computational effort). For example, given $L = 10000$, $p_0 = 0.005$ (i.e., $p_0 \cdot L = 50$), the respective number of all possible candidates (m, r) with $m \in \{1, 2, 5, 10, 25, 50\}$ and

$r \in \{1, 2, 3, \dots, \frac{50}{m}\}$ is

$$\frac{50}{1} + \frac{50}{2} + \frac{50}{5} + \frac{50}{10} + \frac{50}{25} + \frac{50}{50} = 50 + 25 + 10 + 5 + 2 + 1 = 93.$$

To sum up, the proposed brute-force search aims to systematically enumerate all possible candidates (m, r) and to select the one which minimizes the ANU.

5 Performance study

5.1 On-target performance

In this Section, we perform the on-target performance study by considering various values of p_0 , N , m for $r = 1, 2, 4, 8$ and $\text{FAR}_0 = 0.01, 0.05, 0.1$. We focus on the one-sided NBE control chart by considering only the design of the lower control limit LCL_{NH} . The obtained results are shown in Tables 1–4.

For each investigated scenario, Tables 1–4 can be summarized as follows:

- The parameter d_l generally decreases with an increase in N , FAR_0 , and p_0 . Additionally, the values of d_l are increasing with r .
- In general (for $r > 1$), we observe a decreasing value of LCL_{NH} for increasing values of N (converging to LCL_{NB} for $N \rightarrow \infty$). This effect is more evident for large values of r and small values of p_0 . Thus, the negative hypergeometric NBE-chart is more sensitive than its negative binomial counterpart, in particular for small values of N in combination with small values of p_0 . Additionally, there is a decrease in LCL_{NH} when p_0 increases and/or FAR_0 decreases and/or r decreases.
- The obtained values of FAR_{NH} are very close to the nominal value FAR_0 in many cases; in particular, FAR_{NH} varies within the intervals: $[0.008, 0.01]$ for $\text{FAR}_0 = 0.01$, $[0.0414, 0.05]$ for $\text{FAR}_0 = 0.05$ and $[0.0845, 0.1]$ for $\text{FAR}_0 = 0.1$.

As mentioned in Section 4.2, FAR is inferiorly bounded by $\text{FAR}_{\min} = p_0^r$. Therefore, FAP is in turn inferiorly bounded by $\text{FAP}_{\min} = 1 - (1 - p_0^r)^m$. Table 5 shows the values of the lower bound FAP_{\min} for different values of p_0, m, r .

It is worth noting that couples (FAR_0, m) with larger values of FAR_0 and/or m can lead to comparatively high values of FAP_0 . For example, if $(\text{FAR}_0, m) = (0.05, 20)$, we obtain $\text{FAP}_0 = 0.6415$. Although this might seem a high false alarm probability FAP , nevertheless finding a right trade-off between this measure and the detection probability RSP of an assignable cause is a difficult task in SPM of finite horizon processes. If a practitioner fixes a too small nominal value for FAR_0 , for example $\text{FAR}_0 = 0.01$, then the detection probability of the control chart by the end of the production run would be too small due to a lower LCL and, consequently, a poor power (i.e., worse out-of-target performance). For this reason, larger values of FAR should be accounted for by practitioners. To avoid a too bad on-target performance, we suggest to fix the nominal $\text{FAR}_0 = 0.05$ for the design of the NBE-chart since this value seems to meet a good trade-off between the on-target and the out-of-target performance. Of course, choosing different values of m can affect FAP .

Table 1: On-target performance with $r = 1$ and $\text{FAR}_0 = 0.01, 0.05, 0.1$

p_0	$N = 100$	$N = 200$	$N = 500$	$N = 1000$	$N = 2000$	$N = 5000$	$N = 10000$	$N = 100000$	$N \rightarrow \infty$	
$\text{FAR}_0 = 0.01$										
d_l	0.001	–	–	–	1.6991	1.3919	1.1683	1.0828	0.9992	0.9895
	0.005	–	1.6888	1.3930	1.1654	1.0804	1.0257	1.0068	0.9894	0.9875
	0.010	1.6802	1.3824	1.1761	1.0894	1.0322	1.0041	0.9946	0.9859	0.9950
	0.050	–	–	–	–	–	–	–	–	–
LCL_{NH}	0.001	–	–	–	10	11	11	11	11	11
	0.005	–	3	3	3	3	3	3	3	3
	0.010	2	2	2	2	2	2	2	2	2
	0.050	–	–	–	–	–	–	–	–	–
FAR_{NH}	0.001	–	–	–	0.0090	0.0100	0.0100	0.0100	0.0100	0.0100
	0.005	–	0.0100	0.0080	0.0100	0.0100	0.0100	0.0100	0.0100	0.0100
	0.010	0.0100	0.0100	0.0100	0.0100	0.0100	0.0100	0.0100	0.0100	0.0100
	0.050	–	–	–	–	–	–	–	–	–
$\text{FAR}_0 = 0.05$										
d_l	0.001	–	–	–	1.5571	1.3071	1.1101	1.0334	0.9574	0.9485
	0.005	–	1.5675	1.3080	1.1085	1.0320	0.9824	0.9651	0.9492	0.9474
	0.010	1.5416	1.2973	1.1048	1.0289	0.9880	0.9623	0.9536	0.9456	0.9447
	0.050	1.0751	1.0034	0.9565	0.9402	0.9318	0.9268	0.9251	0.9236	0.9234
LCL_{NH}	0.001	–	–	–	51	51	52	52	52	52
	0.005	–	10	13	11	11	11	11	11	11
	0.010	6	6	6	6	6	6	6	6	6
	0.050	2	2	2	2	2	2	2	2	2
FAR_{NH}	0.001	–	–	–	0.0500	0.0494	0.0500	0.0499	0.0498	0.0497
	0.005	–	0.0450	0.0475	0.0491	0.0490	0.0489	0.0489	0.0489	0.0489
	0.010	0.0500	0.0495	0.0492	0.0491	0.0491	0.0490	0.0490	0.0490	0.0490
	0.050	0.0500	0.0500	0.0500	0.0500	0.0500	0.0500	0.0500	0.0500	0.0500
$\text{FAR}_0 = 0.1$										
d_l	0.001	–	–	–	1.3874	1.1967	1.0348	0.9695	0.9023	0.8944
	0.005	–	1.3943	1.1976	1.0374	0.9717	0.9282	0.9129	0.8938	0.8922
	0.010	1.4030	1.1910	1.0336	0.9684	0.9326	0.9101	0.9023	0.8953	0.8945
	0.050	1.0026	0.9417	0.9011	0.8868	0.8795	0.8751	0.8736	0.8722	0.8721
LCL_{NH}	0.001	–	–	–	100	103	105	105	106	106
	0.005	–	20	26	21	21	21	21	22	22
	0.010	10	11	11	11	11	11	11	11	11
	0.050	3	3	3	3	3	3	3	3	3
FAR_{NH}	0.001	–	–	–	0.0990	0.0994	0.0998	0.0993	0.0998	0.0997
	0.005	–	0.0950	0.0976	0.0963	0.0958	0.0956	0.0955	0.0999	0.0999
	0.010	0.0900	0.0977	0.0965	0.0960	0.0958	0.0957	0.0957	0.0956	0.0956
	0.050	0.0980	0.0977	0.0976	0.0975	0.0975	0.0975	0.0975	0.0975	0.0975

Table 2: On-target performance with $r = 2$ and $\text{FAR}_0 = 0.01, 0.05, 0.1$

p_0	$N = 100$	$N = 200$	$N = 500$	$N = 1000$	$N = 2000$	$N = 5000$	$N = 10000$	$N = 100000$	$N \rightarrow \infty$	
$\text{FAR}_0 = 0.01$										
d_l	0.001	–	–	–	–	2.4041	1.6878	1.4937	1.3274	1.3095
	0.005	–	–	2.4037	1.6853	1.4935	1.3827	1.3451	1.3116	1.3079
	0.010	–	2.4032	1.6905	1.4977	1.4014	1.3449	1.3262	1.3095	1.3076
	0.050	–	–	–	–	–	–	–	–	–
LCL_{NH}	0.001	–	–	–	–	201	164	156	150	149
	0.005	–	–	51	34	32	31	31	31	31
	0.010	–	21	17	16	16	16	16	16	16
	0.050	–	–	–	–	–	–	–	–	–
FAR_{NH}	0.001	–	–	–	–	0.0100	0.0099	0.0099	0.0099	0.0099
	0.005	–	–	0.0098	0.0099	0.0097	0.0095	0.0097	0.0099	0.0099
	0.010	–	0.0095	0.0091	0.0088	0.0092	0.0095	0.0096	0.0096	0.0096
	0.050	–	–	–	–	–	–	–	–	–
$\text{FAR}_0 = 0.05$										
d_l	0.001	–	–	–	–	1.8800	1.4419	1.3023	1.1773	1.1631
	0.005	–	–	1.8771	1.4434	1.3044	1.2185	1.1925	1.1656	1.1626
	0.010	–	1.8715	1.4426	1.2992	1.2328	1.1881	1.1805	1.1670	1.1655
	0.050	1.4133	1.3119	1.2207	1.1907	1.1757	1.1667	1.1638	1.1611	1.1608
LCL_{NH}	0.001	–	–	–	–	448	383	369	357	356
	0.005	–	–	113	77	74	73	72	72	72
	0.010	–	46	39	38	37	37	36	36	36
	0.050	9	8	8	8	8	8	8	8	8
FAR_{NH}	0.001	–	–	–	–	0.0499	0.0499	0.0500	0.0498	0.0498
	0.005	–	–	0.0498	0.0491	0.0489	0.0496	0.0489	0.0494	0.0495
	0.010	–	0.0497	0.0486	0.0497	0.0489	0.0498	0.0476	0.0478	0.0454
	0.050	0.0499	0.0414	0.0432	0.0438	0.0441	0.0443	0.0443	0.0444	0.0444
$\text{FAR}_0 = 0.1$										
d_l	0.001	–	–	–	–	1.4874	1.2409	1.1433	1.0489	1.0378
	0.005	–	–	1.4864	1.2410	1.1424	1.0817	1.0584	1.0409	1.0385
	0.010	–	1.4887	1.2397	1.1458	1.0883	1.0611	1.0494	1.0388	1.0376
	0.050	1.2414	1.1281	1.1008	1.0764	1.0642	1.0568	1.0544	1.0522	1.0519
LCL_{NH}	0.001	–	–	–	–	633	562	546	534	533
	0.005	–	–	159	113	110	108	108	107	107
	0.010	–	64	57	55	55	54	54	54	54
	0.050	12	12	11	11	11	11	11	11	11
FAR_{NH}	0.001	–	–	–	–	0.0997	0.0999	0.0998	0.0999	0.1000
	0.005	–	–	0.0994	0.0992	0.0995	0.0990	0.0998	0.0990	0.0991
	0.010	–	0.0981	0.0988	0.0975	0.0998	0.0979	0.0983	0.0987	0.0956
	0.050	0.0919	0.0973	0.0845	0.0853	0.0857	0.0860	0.0861	0.0861	0.0861

Table 3: On-target performance with $r = 4$ and $\text{FAR}_0 = 0.01, 0.05, 0.1$

p_0	$N = 100$	$N = 200$	$N = 500$	$N = 1000$	$N = 2000$	$N = 5000$	$N = 10000$	$N = 100000$	$N \rightarrow \infty$	
$\text{FAR}_0 = 0.01$										
d_l	0.001	-	-	-	-	-	2.4952	1.9472	1.6198	1.5883
	0.005	-	-	-	2.4932	1.9474	1.7190	1.6520	1.5936	1.5890
	0.010	-	-	2.4907	1.9459	1.7531	1.6509	1.6190	1.5915	1.5880
	0.050	-	-	-	-	-	-	-	-	-
LCL_{NH}	0.001	-	-	-	-	-	1112	934	834	825
	0.005	-	-	-	224	188	174	170	167	166
	0.010	-	-	113	95	89	86	85	84	84
	0.050	-	-	-	-	-	-	-	-	-
FAR_{NH}	0.001	-	-	-	-	-	0.0100	0.0100	0.0100	0.0100
	0.005	-	-	-	0.0100	0.0099	0.0099	0.0099	0.0100	0.0098
	0.010	-	-	0.0100	0.0099	0.0099	0.0099	0.0099	0.0098	0.0098
	0.050	-	-	-	-	-	-	-	-	-
$\text{FAR}_0 = 0.05$										
d_l	0.001	-	-	-	-	-	1.8192	1.5380	1.3375	1.3167
	0.005	-	-	-	1.8183	1.5396	1.4014	1.3589	1.3210	1.3158
	0.010	-	-	1.8145	1.5408	1.4231	1.3598	1.3379	1.3192	1.3166
	0.050	1.7953	1.5510	1.3898	1.3618	1.3345	1.3186	1.3133	1.3086	1.3081
LCL_{NH}	0.001	-	-	-	-	-	1714	1502	1379	1368
	0.005	-	-	-	344	301	284	279	275	275
	0.010	-	-	173	151	144	140	139	138	138
	0.050	36	31	30	29	29	29	29	29	29
FAR_{NH}	0.001	-	-	-	-	-	0.0499	0.0500	0.0499	0.0500
	0.005	-	-	-	0.0498	0.0495	0.0497	0.0496	0.0497	0.0500
	0.010	-	-	0.0499	0.0491	0.0494	0.0492	0.0494	0.0494	0.0495
	0.050	0.0495	0.0455	0.0493	0.0466	0.0478	0.0486	0.0488	0.0490	0.0491
$\text{FAR}_0 = 0.1$										
d_l	0.001	-	-	-	-	-	1.4059	1.2678	1.1416	1.1276
	0.005	-	-	-	1.4078	1.2690	1.1849	1.1546	1.1292	1.1278
	0.010	-	-	1.4088	1.2659	1.1950	1.1549	1.1402	1.1276	1.1256
	0.050	1.3942	1.2562	1.1832	1.1692	1.1486	1.1365	1.1325	1.1290	1.1286
LCL_{NH}	0.001	-	-	-	-	-	2082	1877	1757	1746
	0.005	-	-	-	417	376	359	355	351	350
	0.010	-	-	209	189	182	178	177	176	176
	0.050	43	39	37	36	36	36	36	36	36
FAR_{NH}	0.001	-	-	-	-	-	0.1000	0.1000	0.0999	0.0999
	0.005	-	-	-	0.0993	0.0994	0.0993	0.0999	0.1000	0.0995
	0.010	-	-	0.0988	0.0996	0.0999	0.0994	0.0997	0.0997	0.0998
	0.050	0.0975	0.0985	0.0961	0.0922	0.0940	0.0951	0.0954	0.0957	0.0958

Table 4: On-target performance with $r = 8$ and $\text{FAR}_0 = 0.01, 0.05, 0.1$

p_0	$N = 100$	$N = 200$	$N = 500$	$N = 1000$	$N = 2000$	$N = 5000$	$N = 10000$	$N = 100000$	$N \rightarrow \infty$
$\text{FAR}_0 = 0.01$									
d_l	0.001	–	–	–	–	–	2.6368	1.8524	1.8008
	0.005	–	–	–	–	2.6360	2.0309	1.9078	1.8006
	0.010	–	–	–	2.6331	2.1025	1.9069	1.8535	1.8015
	0.050	–	–	–	–	–	–	–	–
LCL_{NH}	0.001	–	–	–	–	–	3885	2970	2909
	0.005	–	–	–	–	779	639	609	584
	0.010	–	–	–	391	329	306	299	294
	0.050	–	–	–	–	–	–	–	–
FAR_{NH}	0.001	–	–	–	–	–	0.0100	0.0100	0.0100
	0.005	–	–	–	–	0.0100	0.0099	0.0099	0.0100
	0.010	–	–	–	0.0100	0.0097	0.0099	0.0098	0.0100
	0.050	–	–	–	–	–	–	–	–
$\text{FAR}_0 = 0.05$									
d_l	0.001	–	–	–	–	–	1.8213	1.4502	1.4209
	0.005	–	–	–	–	1.8214	1.5478	1.4804	1.4260
	0.010	–	–	–	1.8205	1.5833	1.4804	1.4513	1.4213
	0.050	–	1.8381	1.5498	1.4847	1.4479	1.4350	1.4248	1.4157
LCL_{NH}	0.001	–	–	–	–	–	4933	4045	3983
	0.005	–	–	–	–	988	853	824	798
	0.010	–	–	–	495	436	413	406	401
	0.050	–	100	87	84	83	82	82	82
FAR_{NH}	0.001	–	–	–	–	–	0.0500	0.0500	0.0499
	0.005	–	–	–	–	0.0498	0.0497	0.0499	0.0500
	0.010	–	–	–	0.0497	0.0496	0.0498	0.0495	0.0499
	0.050	–	0.0470	0.0481	0.0479	0.0488	0.0481	0.0488	0.0495
$\text{FAR}_0 = 0.1$									
d_l	0.001	–	–	–	–	–	1.3762	1.1999	1.1822
	0.005	–	–	–	–	1.3770	1.2544	1.2181	1.1859
	0.010	–	–	–	1.3752	1.2727	1.2174	1.1995	1.1834
	0.050	–	1.3605	1.2498	1.2204	1.1986	1.1940	1.1864	1.1789
LCL_{NH}	0.001	–	–	–	–	–	5505	4714	4658
	0.005	–	–	–	–	1102	983	956	935
	0.010	–	–	–	552	500	479	473	468
	0.050	–	112	100	97	96	95	95	95
FAR_{NH}	0.001	–	–	–	–	–	0.0999	0.0999	0.1000
	0.005	–	–	–	–	0.0995	0.0998	0.0997	0.0998
	0.010	–	–	–	0.0995	0.0997	0.0996	0.0996	0.0997
	0.050	–	0.0993	0.0986	0.0970	0.0980	0.0965	0.0975	0.0985

Table 5: Minimum values of FAP (FAP_{\min}) given $r = 1, 2, 4, 8$ and $\text{FAR}_0 = \text{FAR}_{\min} = p_0^r$

p_0	$m = 10$	$r = 1$			$r = 2$			$r = 4$			$r = 8$		
		$m = 10$	$m = 20$	$m = 50$	$m = 10$	$m = 20$	$m = 50$	$m = 10$	$m = 20$	$m = 50$	$m = 10$	$m = 20$	$m = 50$
0.001	0.0100	0.0198	0.0488	0.0000	0.0000	0.0000	0.0000	0.0000	0.0000	0.0000	0.0000	0.0000	
0.005	0.0489	0.0954	0.2217	0.0002	0.0005	0.0012	0.0000	0.0000	0.0000	0.0000	0.0000	0.0000	
0.010	0.0956	0.1821	0.3950	0.0010	0.0020	0.0050	0.0000	0.0000	0.0000	0.0000	0.0000	0.0000	
0.050	0.4013	0.6415	0.9231	0.0247	0.0488	0.1176	0.0001	0.0001	0.0003	0.0000	0.0000	0.0000	
0.100	0.6513	0.8784	0.9948	0.0956	0.1821	0.3950	0.0010	0.0020	0.0050	0.0000	0.0000	0.0000	

5.2 Out-of-target performance

In this Section, we discuss the out-of-target performance study, see Tables 6–9. Investigating:

- lot size $L \in \{1000, 2000, 5000, 10000, 100000\}$;
- target fraction nonconforming $p_0 \in \{0.001, 0.005, 0.01, 0.05\}$;

- shift size $\delta \in \{0.001, 0.002, 0.01, 0.02\}$;
- scheduled inspection after the process change-point $s \in \{1, \lfloor \frac{m}{2} + 1 \rfloor\}$.

We design a sampling plan $(m, r, \text{LCL}_{\text{NH}})$ (first row of each cell in Tables 6–9) for each scenario using $\text{FAR}_0 = 0.05$ and give, in addition, the couples $(\text{FAR}_{\text{NH}}, \beta_{\text{NH}}^*)$ (second row of each cell in Tables 6–9) and the values of out-of-target performance measures (RSP, ANU) (third row of each cell in Tables 6–9). As in Section 5.1, we focus on the one-sided NBE control chart by considering only LCL_{NH} .

The findings of Tables 6–9 can be summarized as follows:

- The optimal design couples (m, r) that minimize ANU are in general intermediate solutions mostly close to the condition $(m, r) = (Lp_0, 1)$ for small target values of p_0 (0.001, 0.005), and converging to small values of m and large values of r for large target values of p_0 (0.01, 0.05) in combination with small shifts δ (0.001, 0.002).
- Given p_0 and δ , the value of LCL_{NH} mostly remains the same (e.g., $\text{LCL}_{\text{NH}} = 51$ for $p_0 = 0.001$, $\delta = 0.001$) for various lot sizes L .
- RSP is, in general, increasing with p_0, δ, L or remains unchanged (e.g., $\text{RSP} = 0.2651$ for $p_0 = 0.001$, $\delta = 0.002$, $L = 2000$ and $\text{RSP} = 1$ for $p_0 = 0.005$, $\delta = 0.01$, $L = 5000$).
- ANU is, in general, decreasing with p_0, δ or remains unchanged. In contrast, the values of ANU are mostly increasing with increasing L , apart from some exceptions (e.g., $p_0 = 0.001$, $\delta = 0.01$, $L = 10000$) due to the discreteness of the underlying distribution.
- Sampling plans $(m, r, \text{LCL}_{\text{NH}})$ show a tendency to be the same for $s = 1$ and $s = \lfloor \frac{m}{2} + 1 \rfloor$, with lower values of RSP and ANU for $s = \lfloor \frac{m}{2} + 1 \rfloor$. Considering the high production volume scenario $L = 100000$, sampling plans with corresponding values of $\text{FAR}_{\text{NH}}, \beta_{\text{NH}}^*$, RSP, and ANU are the same for $s = 1$ and $s = \lfloor \frac{m}{2} + 1 \rfloor$.
- The inspection lot size N can increase with L , in particular for $p_0 \leq 0.005$ and $\delta \leq 0.002$. Considering larger values of p_0 , there are less changes in N for an increasing value of L .

Summarizing, it should be noted that the selection of the optimal sampling plans given in Tables 6–9 strongly depends on the production lot size L : on the one hand, sampling plans based on larger values of L are not feasible for low-volume production of small batches of customized units. On the other hand, sampling plans based on lower values of L are not optimal for high-volume production with frequent changeovers.

To carry out a quantitative comparison in terms of ANU with the negative binomial NBE-chart, the sampling plans based on the negative binomial distribution are shown in Tables 10–13 for the same scenarios as in Tables 6–9. These sampling plans are obtained via approximation of LCL_{NH} by LCL_{NB} and PF_{NH} by PF_{NB} . The findings of Tables 10–13 can be classified into two categories:

1. For $L \leq 5000$ in combination with $\delta \geq 0.01$ as well as for $L \geq 10000$, couples (m, r) generally differ from the respective negative hypergeometric case and the values of ANU are larger for the negative binomial NBE-chart.
2. Otherwise, couples (m, r) are the same as in the respective negative hypergeometric case with

- $LCL_{NB} > LCL_{NH}$ for $r = 1$, which can lead to slightly lower, equal or higher values of ANU
- $LCL_{NB} < LCL_{NH}$ for $r \geq 2$, which mostly leads to larger values of ANU for the negative binomial NBE-chart

Summarizing, the negative binomial NBE-chart has a worse out-of-target performance than the negative hypergeometric NBE-chart because the values of ANU are generally larger.

Table 6: Sampling plans ($m, r, \text{LCL}_{\text{NH}}$) with ($\text{FAR}_{\text{NH}}, \beta_{\text{NH}}^*$) and respective (RSP, ANU) for $p_0 = 0.001, \text{FAR}_0 = 0.05$

δ	$L = 1000$		$L = 2000$		$L = 5000$		$L = 10000$		$L = 100000$	
	$s = 1$	$s \in \{1, \lfloor \frac{m}{2} + 1 \rfloor\}$	$s = 1$	$s \in \{1, \lfloor \frac{m}{2} + 1 \rfloor\}$	$s = 1$	$s \in \{1, \lfloor \frac{m}{2} + 1 \rfloor\}$	$s = 1$	$s \in \{1, \lfloor \frac{m}{2} + 1 \rfloor\}$	$s = 1$	$s \in \{1, \lfloor \frac{m}{2} + 1 \rfloor\}$
0.001	(1,1,51) (0.05,0.9025) (0.0975,1000)	(1,1,51) (0.05,0.9025) (0.1856,1903)	(2,1,51) (0.05,0.9025) (0.1856,1903)	(2,1,51) (0.05,0.9025) (0.0975,1000)	(5,1,51) (0.05,0.9025) (0.4014,4116)	(5,1,51) (0.05,0.9025) (0.2650,2717)	(2,5,2748) (0.05,0.2626) (0.9310,6314)	(10,1,51) (0.05,0.9025) (0.4014,4116)	(20,5,2748) (0.05,0.2626) (1.6781)	(20,5,2748) (0.05,0.2626) (1.6781)
0.002	(1,1,51) (0.05,0.8572) (0.1428,1000)	(1,1,51) (0.05,0.8572) (0.2651,1858)	(2,1,51) (0.05,0.8572) (0.2651,1858)	(2,1,51) (0.05,0.8572) (0.1428,1000)	(5,1,51) (0.05,0.8572) (0.5371,3763)	(5,1,51) (0.05,0.8572) (0.3700,2593)	(5,2,448) (0.0499,0.5977) (0.9237,4593)	(10,1,51) (0.05,0.8572) (0.52,448)	(25,4,1893) (0.05,0.1025) (1.4457)	(25,4,1893) (0.05,0.1025) (1.4457)
0.01	(1,1,51) (0.05,0.5671) (0.4329,1000)	(1,1,51) (0.05,0.5671) (0.6783,1568)	(2,1,51) (0.05,0.5671) (0.6783,1568)	(2,1,51) (0.05,0.5671) (0.4329,1000)	(5,1,51) (0.05,0.5671) (0.9413,2175)	(5,1,51) (0.05,0.5671) (0.8176,1889)	(5,2,448) (0.0499,0.0275) (1.2057)	(5,2,448) (0.0499,0.0275) (1.2057)	(50,2,448) (0.0499,0.0275) (1.2057)	(50,2,448) (0.0499,0.0275) (1.2057)
0.02	(1,1,51) (0.05,0.3368) (0.6632,1000)	(1,1,51) (0.05,0.3368) (0.8866,1337)	(2,1,51) (0.05,0.3368) (0.8866,1337)	(2,1,51) (0.05,0.3368) (0.6632,1000)	(5,1,51) (0.05,0.3368) (0.9957,1502)	(5,1,51) (0.05,0.3368) (0.9618,1451)	(10,1,51) (0.05,0.3368) (1.1508)	(10,1,51) (0.05,0.3368) (0.9957,1502)	(100,1,51) (0.05,0.3368) (1.1508)	(100,1,51) (0.05,0.3368) (1.1508)

Table 7: Sampling plans ($m, r, \text{LCL}_{\text{NH}}$) with ($\text{FAR}_{\text{NH}}, \beta_{\text{NH}}^*$) and respective (RSP, ANU) for $p_0 = 0.005, \text{FAR}_0 = 0.05$

δ	$L = 1000$		$L = 2000$		$L = 5000$		$L = 10000$		$L = 100000$	
	$s = 1$	$s \in \{1, \lfloor \frac{m}{2} + 1 \rfloor\}$	$s = 1$	$s \in \{1, \lfloor \frac{m}{2} + 1 \rfloor\}$	$s = 1$	$s \in \{1, \lfloor \frac{m}{2} + 1 \rfloor\}$	$s = 1$	$s \in \{1, \lfloor \frac{m}{2} + 1 \rfloor\}$	$s = 1$	$s \in \{1, \lfloor \frac{m}{2} + 1 \rfloor\}$
0.001	(1,5,551) (0.0499,0.8372) (0.1628,1000)	(1,5,551) (0.0499,0.8372) (0.1628,1000)	(2,5,551) (0.0499,0.8372) (0.2991,1838)	(2,5,551) (0.0499,0.8372) (0.1628,1000)	(5,5,551) (0.0499,0.8372) (0.5887,3617)	(5,5,551) (0.0499,0.8372) (0.4132,2539)	(5,10,1484) (0.0499,0.6358) (0.8961,4922)	(10,5,551) (0.0499,0.8372) (0.5887,3617)	(25,20,3445) (0.0497,0.2337) (1.5220)	(25,20,3445) (0.0497,0.2337) (1.5220)
0.002	(1,5,551) (0.0499,0.6842) (0.3158,1000)	(1,5,551) (0.0499,0.6842) (0.5318,1685)	(2,5,551) (0.0499,0.6842) (0.5318,1685)	(2,5,551) (0.0499,0.6842) (0.3158,1000)	(5,5,551) (0.0499,0.6842) (0.8500,2692)	(5,5,551) (0.0499,0.6842) (0.6796,2153)	(5,10,1484) (0.0499,0.2833) (0.9982,2786)	(10,5,551) (0.0499,0.6842) (0.8500,2692)	(50,10,1484) (0.0499,0.2833) (1.2791)	(50,10,1484) (0.0499,0.2833) (1.2791)
0.01	(5,1,10) (0.0450,0.8704) (0.5005,773)	(5,1,10) (0.0450,0.8704) (0.3407,526)	(5,2,90) (0.0491,0.5999) (0.9223,923)	(10,1,10) (0.0450,0.8704) (0.5005,773)	(5,5,551) (0.0499,0.0246) (1,1026)	(5,5,551) (0.0499,0.0246) (1,1026)	(25,2,90) (0.0491,0.5999) (1.1000)	(25,2,90) (0.0491,0.5999) (0.9987,999)	(125,4,380) (0.0500,0.1001) (1,890)	(125,4,380) (0.0500,0.1001) (1,890)
0.02	(5,1,10) (0.0450,0.7925) (0.6875,663)	(5,1,10) (0.0450,0.7925) (0.5023,485)	(5,2,90) (0.0491,0.3083) (0.9972,577)	(5,2,90) (0.0491,0.3083) (0.9707,562)	(25,1,10) (0.0450,0.7925) (0.9972,577)	(25,1,10) (0.0450,0.7925) (0.9514,917)	(25,2,90) (0.0491,0.3083) (1.579)	(25,2,90) (0.0491,0.3083) (1.579)	(250,2,90) (0.0491,0.3083) (1.579)	(250,2,90) (0.0491,0.3083) (1.579)

Table 8: Sampling plans ($m, r, \text{LCL}_{\text{NH}}$) with ($\text{FAR}_{\text{NH}}, \beta_{\text{NH}}^*$) and respective (RSP, ANU) for $p_0 = 0.01$, $\text{FAR}_0 = 0.05$

δ	$L = 1000$		$L = 2000$		$L = 5000$		$L = 10000$		$L = 100000$	
	$s = 1$	$s \in \{1, \lfloor \frac{m}{2} + 1 \rfloor\}$	$s = 1$	$s \in \{1, \lfloor \frac{m}{2} + 1 \rfloor\}$	$s = 1$	$s \in \{1, \lfloor \frac{m}{2} + 1 \rfloor\}$	$s = 1$	$s \in \{1, \lfloor \frac{m}{2} + 1 \rfloor\}$	$s = 1$	$s \in \{1, \lfloor \frac{m}{2} + 1 \rfloor\}$
0.001	(1,10,743) (0.0498,0.8204) (0.1796,1000)	(1,10,743) (0.0498,0.8204) (0.1796,1000)	(2,10,743) (0.0498,0.8204) (0.3269,1821)	(2,10,743) (0.0498,0.8204) (0.1796,1000)	(5,10,743) (0.0498,0.8204) (0.6283,3499)	(5,10,743) (0.0498,0.8204) (0.4478,2494)	(5,20,1724) (0.0499,0.6057) (0.9185,4660)	(5,20,1724) (0.0499,0.6057) (0.6283,3499)	(25,40,3713) (0.0496,0.2071) (1,5045)	(25,40,3713) (0.0496,0.2071) (1,5045)
0.002	(2,5,276) (0.0495,0.8380) (0.2978,919)	(2,5,276) (0.0495,0.8380) (0.162,500)	(4,5,276) (0.0495,0.8380) (0.5069,1565)	(4,5,276) (0.0495,0.8380) (0.2978,919)	(5,10,743) (0.0495,0.8380) (0.8968,2457)	(10,5,276) (0.0495,0.6350) (0.5868,1811)	(5,20,1724) (0.0499,0.2309) (0.9993,2599)	(5,20,1724) (0.0498,0.6350) (0.5968,2457)	(50,20,1724) (0.0499,0.2309) (1,2601)	(50,20,1724) (0.0499,0.2309) (1,2601)
0.01	(2,5,276) (0.0495,0.2595) (0.9327,630)	(10,1,6) (0.0500,0.9020) (0.4029,412)	(4,5,276) (0.0495,0.2595) (0.9955,673)	(4,5,276) (0.0495,0.2595) (0.9327,630)	(10,5,276) (0.0495,0.2595) (0.9988,675)	(10,5,276) (0.0495,0.2595) (0.9988,675)	(20,5,276) (0.0495,0.2595) (1,676)	(20,5,276) (0.0495,0.2595) (1,676)	(200,5,276) (0.0495,0.2595) (1,676)	(200,5,276) (0.0495,0.2595) (1,676)
0.02	(5,2,46) (0.0497,0.5933) (0.9265,456)	(10,1,6) (0.0500,0.8560) (0.5404,376)	(5,4,190) (0.0490,0.0999) (1,445)	(5,4,190) (0.0490,0.0999) (0.9990,444)	(25,2,46) (0.0497,0.5933) (1,492)	(25,2,46) (0.0497,0.5933) (0.9989,492)	(25,4,190) (0.0490,0.0999) (1,445)	(25,4,190) (0.0490,0.0999) (1,445)	(250,4,190) (0.0490,0.1000) (1,445)	(250,4,190) (0.0490,0.1000) (1,445)

Table 9: Sampling plans ($m, r, \text{LCL}_{\text{NH}}$) with ($\text{FAR}_{\text{NH}}, \beta_{\text{NH}}^*$) and respective (RSP, ANU) for $p_0 = 0.05$, $\text{FAR}_0 = 0.05$

δ	$L = 1000$		$L = 2000$		$L = 5000$		$L = 10000$		$L = 100000$	
	$s = 1$	$s \in \{1, \lfloor \frac{m}{2} + 1 \rfloor\}$	$s = 1$	$s \in \{1, \lfloor \frac{m}{2} + 1 \rfloor\}$	$s = 1$	$s \in \{1, \lfloor \frac{m}{2} + 1 \rfloor\}$	$s = 1$	$s \in \{1, \lfloor \frac{m}{2} + 1 \rfloor\}$	$s = 1$	$s \in \{1, \lfloor \frac{m}{2} + 1 \rfloor\}$
0.001	(1,50,944) (0.0492,0.8031) (0.1969,1000)	(1,50,944) (0.0492,0.8031) (0.1969,1000)	(2,50,944) (0.0492,0.8031) (0.3551,1804)	(2,50,944) (0.0492,0.8031) (0.1969,1000)	(5,50,944) (0.0492,0.8031) (0.6660,3382)	(5,50,944) (0.0492,0.8031) (0.4821,2448)	(5,100,1943) (0.0488,0.5762) (0.9365,4420)	(5,100,1943) (0.0488,0.5762) (0.6660,3382)	(50,100,1943) (0.0488,0.5762) (1,4719)	(50,100,1943) (0.0488,0.5762) (1,4719)
0.002	(2,25,445) (0.0475,0.8127) (0.3395,907)	(2,25,445) (0.0475,0.8127) (0.1873,500)	(4,25,445) (0.0475,0.8127) (0.5638,1505)	(4,25,445) (0.0475,0.8127) (0.3395,907)	(5,50,944) (0.0492,0.5808) (0.9339,2228)	(10,25,445) (0.0475,0.8127) (0.6455,1724)	(10,50,944) (0.0492,0.5808) (0.9956,2376)	(10,50,944) (0.0492,0.5808) (0.9339,2228)	(100,50,944) (0.0492,0.5808) (1,2386)	(100,50,944) (0.0492,0.5808) (1,2386)
0.01	(5,10,150) (0.0486,0.6310) (0.9000,488)	(10,5,56) (0.0462,0.8444) (0.5708,367)	(5,20,346) (0.0480,0.2222) (0.9995,514)	(10,10,150) (0.0486,0.6310) (0.9000,488)	(25,10,150) (0.0486,0.6310) (1,542)	(25,10,150) (0.0486,0.6310) (0.9975,541)	(25,20,346) (0.0480,0.2222) (1,515)	(25,20,346) (0.0480,0.2222) (1,515)	(250,20,346) (0.0480,0.2222) (1,515)	(250,20,346) (0.0480,0.2222) (1,515)
0.02	(5,10,150) (0.0486,0.2679) (0.9986,273)	(5,10,150) (0.0486,0.2679) (0.9808,268)	(10,10,150) (0.0486,0.2679) (1,274)	(10,10,150) (0.0486,0.2679) (0.9986,273)	(25,10,150) (0.0486,0.2679) (1,274)	(25,10,150) (0.0486,0.2679) (1,274)	(50,10,150) (0.0486,0.2679) (1,274)	(50,10,150) (0.0486,0.2679) (1,274)	(500,10,150) (0.0486,0.2679) (1,274)	(500,10,150) (0.0486,0.2679) (1,274)

Table 10: Sampling plans ($m, r, \text{LCL}_{\text{NB}}$) with ($\text{FAR}_{\text{NB}}, \beta_{\text{NB}}^*$) and respective (RSP, ANU) for $p_0 = 0.001$, $\text{FAR}_0 = 0.05$

δ	$L = 1000$		$L = 2000$		$L = 5000$		$L = 10000$		$L = 100000$	
	$s = 1$	$s \in \{1, \lfloor \frac{m}{2} + 1 \rfloor\}$	$s = 1$	$s \in \{1, \lfloor \frac{m}{2} + 1 \rfloor\}$	$s = 1$	$s \in \{1, \lfloor \frac{m}{2} + 1 \rfloor\}$	$s = 1$	$s \in \{1, \lfloor \frac{m}{2} + 1 \rfloor\}$	$s = 1$	$s \in \{1, \lfloor \frac{m}{2} + 1 \rfloor\}$
0.001	(1,1,52) (0.0497,0.9029) (0.0971,1000)	(1,1,52) (0.0497,0.9029) (0.0971,1000)	(2,1,52) (0.0497,0.9029) (0.1847,1903)	(2,1,52) (0.0497,0.9029) (0.0971,1000)	(5,1,52) (0.0497,0.9029) (0.3998,4120)	(5,1,52) (0.0497,0.9029) (0.2638,2719)	(10,1,52) (0.0497,0.9029) (0.6398,6592)	(10,1,52) (0.0497,0.9029) (0.3998,4120)	(100,1,52) (0.0497,0.9029) (1,10302)	(100,1,52) (0.0497,0.9029) (1,10240)
0.002	(1,1,52) (0.0497,0.8579) (0.1421,1000)	(1,1,52) (0.0497,0.8579) (0.1421,1000)	(2,1,52) (0.0497,0.8579) (0.2640,1858)	(2,1,52) (0.0497,0.8579) (0.1421,1000)	(5,1,52) (0.0497,0.8579) (0.5352,3768)	(5,1,52) (0.0497,0.8579) (0.3685,2594)	(10,1,52) (0.0497,0.8579) (0.7840,5519)	(10,1,52) (0.0497,0.8579) (0.5352,3768)	(25,4,1368) (0.05,0.4137) (1,6822)	(25,4,1368) (0.05,0.4137) (1,6822)
0.01	(1,1,52) (0.0497,0.5689) (0.4311,1000)	(1,1,52) (0.0497,0.5689) (0.4311,1000)	(2,1,52) (0.0497,0.5689) (0.6764,1569)	(2,1,52) (0.0497,0.5689) (0.4311,1000)	(5,1,52) (0.0497,0.5689) (0.9404,2182)	(5,1,52) (0.0497,0.5689) (0.8159,1893)	(10,1,52) (0.0497,0.5689) (0.9404,2182)	(10,1,52) (0.0497,0.5689) (0.9404,2182)	(50,2,356) (0.0498,0.0975) (1,2216)	(50,2,356) (0.0498,0.0975) (1,2216)
0.02	(1,1,52) (0.0497,0.3388) (0.6612,1000)	(1,1,52) (0.0497,0.3388) (0.6612,1000)	(2,1,52) (0.0497,0.3388) (0.8852,1339)	(2,1,52) (0.0497,0.3388) (0.6612,1000)	(5,1,52) (0.0497,0.3388) (0.9955,1506)	(5,1,52) (0.0497,0.3388) (0.9611,1454)	(10,1,52) (0.0497,0.3388) (1,1513)	(10,1,52) (0.0497,0.3388) (0.9955,1506)	(100,1,52) (0.0497,0.3388) (1,1512)	(100,1,52) (0.0497,0.3388) (1,1512)

Table 11: Sampling plans ($m, r, \text{LCL}_{\text{NB}}$) with ($\text{FAR}_{\text{NB}}, \beta_{\text{NB}}^*$) and respective (RSP, ANU) for $p_0 = 0.005$, $\text{FAR}_0 = 0.05$

δ	$L = 1000$		$L = 2000$		$L = 5000$		$L = 10000$		$L = 100000$	
	$s = 1$	$s \in \{1, \lfloor \frac{m}{2} + 1 \rfloor\}$	$s = 1$	$s \in \{1, \lfloor \frac{m}{2} + 1 \rfloor\}$	$s = 1$	$s \in \{1, \lfloor \frac{m}{2} + 1 \rfloor\}$	$s = 1$	$s \in \{1, \lfloor \frac{m}{2} + 1 \rfloor\}$	$s = 1$	$s \in \{1, \lfloor \frac{m}{2} + 1 \rfloor\}$
0.001	(1,5,396) (0.05,0.9085) (0.0915,1000)	(1,5,396) (0.05,0.9085) (0.0915,1000)	(2,5,396) (0.05,0.9085) (0.1747,1909)	(2,5,396) (0.05,0.9085) (0.0915,1000)	(5,5,396) (0.05,0.9085) (0.3812,4165)	(5,5,396) (0.05,0.9085) (0.2502,2734)	(10,5,396) (0.05,0.9085) (0.6171,6742)	(10,5,396) (0.05,0.9085) (0.3812,4165)	(100,5,396) (0.05,0.9085) (0.9999,10923)	(100,5,396) (0.05,0.9085) (0.9918,10834)
0.002	(1,5,396) (0.05,0.8538) (0.1462,1000)	(1,5,396) (0.05,0.8538) (0.1462,1000)	(2,5,396) (0.05,0.8538) (0.2711,1854)	(2,5,396) (0.05,0.8538) (0.1462,1000)	(5,5,396) (0.05,0.8538) (0.5464,3737)	(5,5,396) (0.05,0.8538) (0.3777,2583)	(10,5,396) (0.05,0.8538) (0.7943,5431)	(10,5,396) (0.05,0.8538) (0.5464,3737)	(100,5,396) (0.05,0.8538) (1,6838)	(100,5,396) (0.05,0.8538) (0.9996,6835)
0.01	(5,1,11) (0.0489,0.8597) (0.5303,757)	(5,1,11) (0.0489,0.8597) (0.3645,520)	(10,1,11) (0.0489,0.8597) (0.7794,1112)	(10,1,11) (0.0489,0.8597) (0.5303,757)	(25,1,11) (0.0489,0.8597) (0.9771,1394)	(25,1,11) (0.0489,0.8597) (0.8598,1226)	(25,2,72) (0.0495,0.7117) (0.9998,1388)	(25,2,72) (0.0495,0.7117) (0.9880,1371)	(125,4,275) (0.05,0.4107) (1,1358)	(125,4,275) (0.05,0.4107) (1,1358)
0.02	(5,1,11) (0.0489,0.7763) (0.7180,643)	(5,1,11) (0.0489,0.7763) (0.5321,476)	(5,2,72) (0.0495,0.4674) (0.9777,735)	(10,1,11) (0.0489,0.7763) (0.7180,643)	(25,1,11) (0.0489,0.7763) (0.9982,893)	(25,1,11) (0.0489,0.7763) (0.9628,861)	(25,2,72) (0.0495,0.4674) (1,751)	(25,2,72) (0.0495,0.4674) (0.9999,751)	(250,2,72) (0.0495,0.4674) (1,751)	(250,2,72) (0.0495,0.4674) (1,751)

Table 12: Sampling plans ($m, r, \text{LCL}_{\text{NB}}$) with $(\text{FAR}_{\text{NB}}, \beta_{\text{NB}}^*)$ and respective (RSP, ANU) for $p_0 = 0.01$, $\text{FAR}_0 = 0.05$

δ	$L = 1000$		$L = 2000$		$L = 5000$		$L = 10000$		$L = 100000$	
	$s = 1$	$s \in \{1, \lfloor \frac{m}{2} + 1 \rfloor\}$	$s = 1$	$s \in \{1, \lfloor \frac{m}{2} + 1 \rfloor\}$	$s = 1$	$s \in \{1, \lfloor \frac{m}{2} + 1 \rfloor\}$	$s = 1$	$s \in \{1, \lfloor \frac{m}{2} + 1 \rfloor\}$	$s = 1$	$s \in \{1, \lfloor \frac{m}{2} + 1 \rfloor\}$
0.001	(1,10,545)	(1,10,545)	(2,10,545)	(2,10,545)	(5,10,545)	(2,25,1742)	(10,10,545)	(10,10,545)	(100,10,545)	(100,10,545)
	(0.0498,0.9183)	(0.0498,0.9183)	(0.0498,0.9183)	(0.0498,0.9183)	(0.0498,0.9183)	(0.0499,0.8877)	(0.0498,0.9183)	(0.0498,0.9183)	(0.0498,0.9183)	(0.0498,0.9183)
0.002	(0.0817,1000)	(0.0817,1000)	(0.1567,1919)	(0.0817,1000)	(0.3469,4248)	(0.1123,2500)	(0.5735,7021)	(0.3469,4248)	(0.9998,12239)	(0.9998,12239)
	(2.5,199)	(2.5,199)	(4.5,199)	(4.5,199)	(10.5,199)	(10.5,199)	(20.5,199)	(20.5,199)	(200.5,199)	(200.5,199)
0.01	(0.05,0.9083)	(0.05,0.9083)	(0.05,0.9083)	(0.05,0.9083)	(0.05,0.9083)	(0.05,0.9083)	(0.05,0.9083)	(0.05,0.9083)	(0.05,0.9083)	(0.05,0.9083)
	(0.1749,955)	(0.0917,500)	(0.3193,1742)	(0.1749,955)	(0.6177,3369)	(0.3817,2082)	(0.8538,4658)	(0.6177,3369)	(1.5454)	(0.9999,5454)
0.02	(10,1.6)	(10,1.6)	(20,1.6)	(20,1.6)	(50,1.6)	(50,1.6)	(100,1.6)	(100,1.6)	(250,4,138)	(250,4,138)
	(0.0490,0.9039)	(0.0490,0.9039)	(0.0490,0.9039)	(0.0490,0.9039)	(0.0490,0.9039)	(0.0490,0.9039)	(0.0490,0.9039)	(0.0490,0.9039)	(0.0495,0.7058)	(0.0495,0.7058)
0.02	(0.6358,662)	(0.3965,413)	(0.8674,903)	(0.6358,662)	(0.9936,1035)	(0.9200,938)	(1.1041)	(0.9936,1035)	(1,1360)	(1,1360)
	(10,1.6)	(10,1.6)	(5,4,138)	(20,1.6)	(10,5,199)	(50,1.6)	(25,4,138)	(25,4,138)	(250,4,138)	(250,4,138)
0.02	(0.0490,0.8587)	(0.0490,0.8587)	(0.0495,0.4091)	(0.0490,0.8587)	(0.5000,0.2891)	(0.0490,0.8587)	(0.0495,0.4091)	(0.0495,0.4091)	(0.0495,0.4091)	(0.0495,0.4091)
	(0.7819,554)	(0.5330,378)	(0.9885,670)	(0.7819,554)	(1.704)	(0.9778,693)	(1.677)	(1.677)	(1,677)	(1,677)

Table 13: Sampling plans ($m, r, \text{LCL}_{\text{NB}}$) with $(\text{FAR}_{\text{NB}}, \beta_{\text{NB}}^*)$ and respective (RSP, ANU) for $p_0 = 0.05$, $\text{FAR}_0 = 0.05$

δ	$L = 1000$		$L = 2000$		$L = 5000$		$L = 10000$		$L = 100000$	
	$s = 1$	$s \in \{1, \lfloor \frac{m}{2} + 1 \rfloor\}$	$s = 1$	$s \in \{1, \lfloor \frac{m}{2} + 1 \rfloor\}$	$s = 1$	$s \in \{1, \lfloor \frac{m}{2} + 1 \rfloor\}$	$s = 1$	$s \in \{1, \lfloor \frac{m}{2} + 1 \rfloor\}$	$s = 1$	$s \in \{1, \lfloor \frac{m}{2} + 1 \rfloor\}$
0.001	(1,50,785)	(1,50,785)	(2,50,785)	(2,50,785)	(5,50,785)	(2,125,2153)	(10,50,785)	(10,50,785)	(100,50,785)	(100,50,785)
	(0.0497,0.9352)	(0.0497,0.9352)	(0.0497,0.9352)	(0.0497,0.9352)	(0.0497,0.9352)	(0.0498,0.9237)	(0.0497,0.9352)	(0.0497,0.9352)	(0.0497,0.9352)	(0.0497,0.9352)
0.002	(0.0648,1000)	(0.0648,1000)	(0.1255,1936)	(0.0648,1000)	(0.2848,4393)	(0.0763,2500)	(0.4885,7534)	(0.2848,4393)	(0.9988,15404)	(0.9988,15404)
	(2.25,352)	(2.25,352)	(4.25,352)	(4.25,352)	(10.25,352)	(10.25,352)	(20.25,352)	(20.25,352)	(200.25,352)	(200.25,352)
0.01	(0.05,0.9285)	(0.05,0.9285)	(0.05,0.9285)	(0.05,0.9285)	(0.05,0.9285)	(0.05,0.9285)	(0.05,0.9285)	(0.05,0.9285)	(0.05,0.9285)	(0.05,0.9285)
	(0.1378,965)	(0.0715,500)	(0.2566,1796)	(0.1378,965)	(0.5236,3664)	(0.3098,2168)	(0.7730,5409)	(0.5236,3664)	(1.6997)	(0.9994,6993)
0.02	(10,5,41)	(10,5,41)	(20,5,41)	(20,5,41)	(50,5,41)	(50,5,41)	(100,5,41)	(100,5,41)	(500,10,111)	(500,10,111)
	(0.0480,0.9104)	(0.0480,0.9104)	(0.0480,0.9104)	(0.0480,0.9104)	(0.0480,0.9104)	(0.0480,0.9104)	(0.0480,0.9104)	(0.0480,0.9104)	(0.0492,0.8753)	(0.0492,0.8753)
0.02	(0.6088,680)	(0.3745,419)	(0.8470,946)	(0.6088,680)	(0.9908,1107)	(0.9043,1010)	(0.9999,1117)	(0.9908,1007)	(1,1604)	(1,1604)
	(10,5,41)	(10,5,41)	(25,4,29)	(25,4,29)	(50,5,41)	(50,5,41)	(125,4,29)	(125,4,29)	(500,10,111)	(500,10,111)
0.02	(0.0480,0.8546)	(0.0480,0.8546)	(0.0491,0.8711)	(0.0491,0.8711)	(0.0480,0.8546)	(0.0480,0.8546)	(0.0491,0.8711)	(0.0491,0.8711)	(0.0492,0.7588)	(0.0492,0.7588)
	(0.7921,545)	(0.5441,375)	(0.9682,602)	(0.8336,518)	(0.9996,688)	(0.9803,675)	(1.621)	(0.9998,621)	(1,829)	(1,829)

6 Illustrative example

In this Section, we illustrate a practical application of the negative hypergeometric NBE-chart using a data set taken from CHAN et al.²⁸, which consists of a total of 8160 inspected units, where 48 units are nonconforming. The positions of the nonconforming units within the data set can be seen in Table 14.

Table 14: Positions of nonconforming units within the data set

113	218	282	505	664	792	963	1110	1184	1341	1547	1733
1808	1861	2030	2186	2337	2569	2704	2889	3063	3263	3373	3433
3559	3809	4021	4206	4472	4517	4833	5032	5325	5375	5553	5729
5988	6338	6424	6692	6996	7201	7227	7314	7578	7703	7879	7963

We are interested to investigate by means of the negative hypergeometric NBE-chart if the fraction nonconforming $p_0 = \frac{48}{8160} \approx 0.0059$ is stable versus time or if there are potential change-points. Thus, we assume the units as a lot of $L = 8160$ units to be produced during a period of H hours. A finite number m of inspections with $m \in \{1, 2, 3, 4, 6, 8, 12, 16, 24, 48\}$, where $L \cdot p_0 = 48$, can be scheduled during the production run. Between two consecutive inspections, $N = \frac{L}{m}$ units with $N \in \{170, \dots, 8160\}$ are produced. At each scheduled inspection j , the samples y_j , $j = 1, \dots, m$, are collected every $h = \frac{H}{m}$ hours from the N units produced between the $(j-1)$ -th and j -th inspection. Given the set of feasible m values, we can define the following inspection plans with maximum feasible r values:

$$(m, r_{\max}, N) = \{(1, 48, 8160), (2, 24, 4080), (3, 16, 2720), (4, 12, 2040), (6, 8, 1360), \\ (8, 6, 1020), (12, 4, 680), (16, 3, 510), (24, 2, 340), (48, 1, 170)\}$$

Here, r_{\max} denotes the maximum feasible number of nonconforming units to trigger a signal from the NBE control chart for a selected value of m in the inspection plan, i.e., $r \in \{1, \dots, r_{\max}\}$. For example, if we choose $(6, 8, 1360)$, then we obtain eight inspection plans, where $m = 6$ and $r \in \{1, \dots, 8\}$ can be varied by minimizing the ANU with an inspection lot size $N = \frac{L}{m} = 1360$. It is worth noting that the two extreme inspection plans $(1, 48, 8160)$ and $(48, 1, 170)$ provide the worst out-of-target and the worst on-target performance, respectively.

If we would like to design an inspection plan by minimizing the value of ANU under a constraint on FAR_0 , we should decide *a priori* the change-point position, e.g., the value of s , and the shift size δ in the fraction nonconforming. Thus, we assume $s \in \{1, \lfloor \frac{m}{2} + 1 \rfloor\}$ and $\delta = \{0.001, 0.002, 0.01, 0.02\}$, and look for the couple (m, r) minimizing the value of ANU. We consider the one-sided case to determine LCL_{NH} for the target false alarm rate $\text{FAR}_0 = 0.05$. The results of this optimization procedure are given in Table 15. In particular, the inspection effort decreases with δ and s , FAR_{NH} meets the constraint on the given FAR_0 , and RSP increases with δ and m . Further, ANU is decreasing with δ and m .

Table 15: Data set example. Inspection plans (m, r, N) for various values of δ with $s = 1$ or $s = \lfloor \frac{m}{2} + 1 \rfloor$, $p_0 = 0.0059$, $FAR_0 = 0.05$

δ	s	(m, r, N)	LCL_{NH}	FAR	β^*	RSP	ANU
0.001	1	(4, 12, 2040)	1591	0.0498	0.6267	0.8458	4622
	5	(8, 6, 1020)	621	0.0500	0.8318	0.5213	3162
0.002	1	(4, 12, 2040)	1591	0.0498	0.2666	0.9949	2768
	5	(8, 6, 1020)	621	0.0500	0.6688	0.7999	2464
0.003	1	(6, 8, 1360)	937	0.0499	0.3074	0.9992	1963
	4	(6, 8, 1360)	937	0.0499	0.3074	0.9709	1907
0.005	1	(8, 6, 1020)	621	0.0500	0.2283	1.0000	1322
	5	(8, 6, 1020)	621	0.0500	0.2283	0.9973	1319
0.008	1	(12, 4, 680)	323	0.0498	0.3074	1.0000	982
	7	(12, 4, 680)	323	0.0498	0.3074	0.9992	981
0.010	1	(16, 3, 510)	189	0.0496	0.3829	1.0000	827
	9	(16, 3, 510)	189	0.0496	0.3829	0.9995	827
0.015	1	(16, 3, 510)	189	0.0496	0.2207	1.0000	655
	9	(16, 3, 510)	189	0.0496	0.2207	1.0000	655
0.020	1	(16, 3, 510)	189	0.0496	0.0863	1.0000	559
	9	(16, 3, 510)	189	0.0496	0.0863	1.0000	559

If the practitioner is interested in the detection of small shifts like $\delta = 0.001$, then s/he should implement the inspection plan (4, 12, 2040) for $s = 1$ and (8, 6, 1020) for $s = \lfloor \frac{m}{2} + 1 \rfloor = 5$, respectively, depending on her/his opinion about when the change-point can occur (e.g., based on prior knowledge, experience, economic aspects). These inspection plans lead to the minimum of ANU, i.e., $ANU = 4622$ and $ANU = 3162$, respectively, among further reasonable inspection plans. In addition, Figures 1–2 show how ANU (y -axis) depends on selecting a particular inspection plan (m, r) , where m is the parameter identifying each curve ($m = 1, 2, 3, 4, 6, 8$, from top to bottom) and r corresponds to the x -axis. The respective optimal inspection plan is circled in Figures 1–2. Note that numerical results are displayed by a line plot instead of a scatter plot for better output illustration.

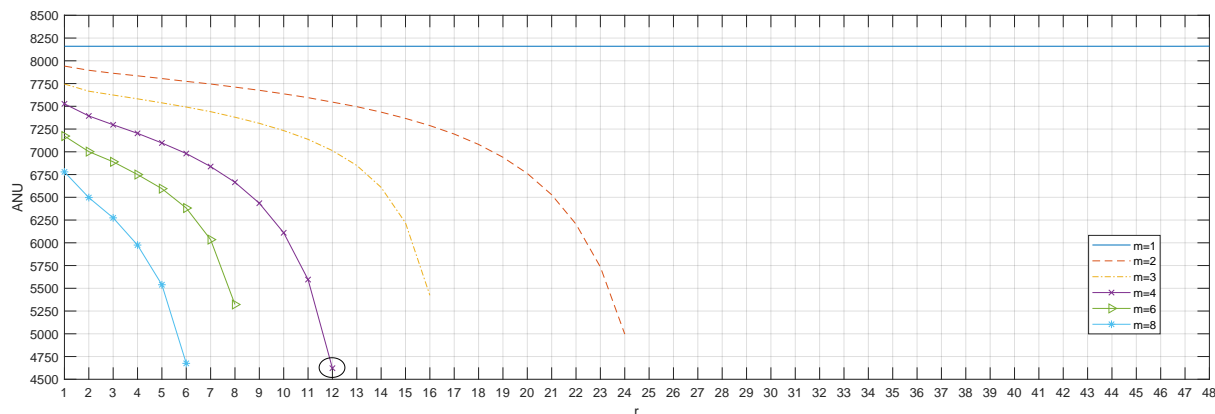


Figure 1: Data set example. Inspection plans (m, r) with respective ANU for $p_0 = 0.0059$, $FAR_0 = 0.05$, $\delta = 0.001$, $s = 1$

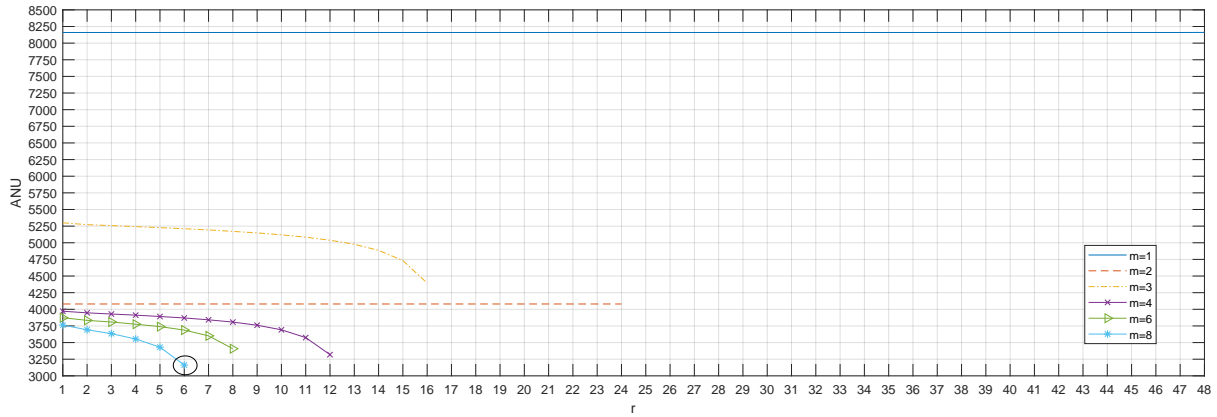


Figure 2: Data set example. Inspection plans (m, r) with respective ANU for $p_0 = 0.0059$, $\text{FAR}_0 = 0.05$, $\delta = 0.001$, $s = \lfloor \frac{m}{2} + 1 \rfloor$

Figure 3 shows an exemplary negative hypergeometric NBE-chart with $\text{CL}_{\text{NH}} = 876$ and $\text{LCL}_{\text{NH}} = 621$ for the optimal inspection plan $(8, 6, 1020)$. The samples y_j , $j = 1, \dots, 8$, are either given by the number of inspected units in the j -th sample until the sixth nonconforming unit occurs or $y_j = N = 1020$ when the inspection of a single inspection lot is finished without finding $r = 6$ nonconforming units. In particular, the sample statistics are $y_1 = 792$, $y_2 = 788$, $y_3 = 1020$, $y_4 = 749$, $y_5 = 1020$, $y_6 = 1020$, $y_7 = 1020$, $y_8 = 739$ (see Table 16, third column block). We obtain $r = 6$ nonconforming units by sampling the 792th unit in the first inspection (6th position in Table 14), the 788th unit in the second inspection (13th position in Table 14), while the third inspection is finished without finding $r = 6$ nonconforming units, and so on.

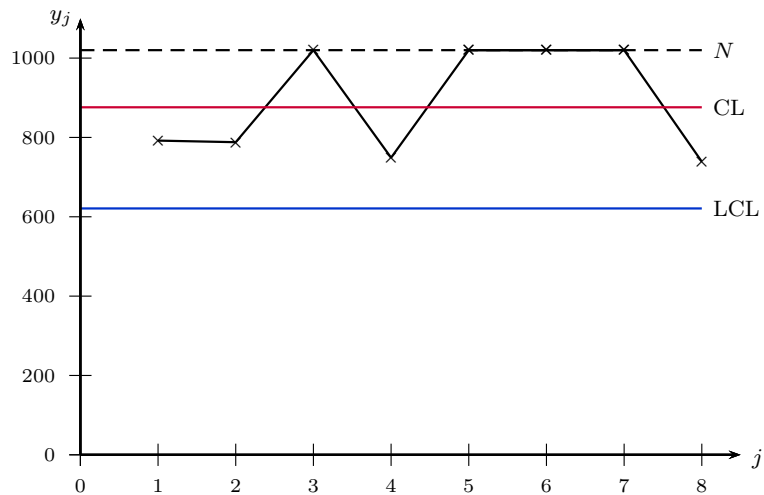


Figure 3: Data set example. Negative hypergeometric NBE-chart for inspection plan $(m, r, N) = (8, 6, 1020)$

In addition, Table 16 shows negative hypergeometric NBE-charts for further optimal inspection plans $(m, r, N) = (4, 12, 2040)$, $(6, 8, 1360)$, $(12, 4, 680)$, $(16, 3, 510)$, which are given in Table 15. A single potential process change-point, where the negative hypergeometric NBE-chart with inspection plan $(16, 3, 510)$ detects sample y_{15} as out of LCL_{NH} (that is, a significant increase in the process fraction nonconforming is declared), is highlighted using a frame-box in Table 16. Analyzing this chart, the process engineer

would search for the assignable cause and adjust the process to decrease the fraction nonconforming.

Table 16: Negative hypergeometric NBE-charts for optimal inspection plans (m, r, N) , given $L = 8160$, $p_0 = 0.0059$, $FAR_0 = 0.05$

(4, 12, 2040) LCL _{NH} = 1591 CL _{NH} = 1884			(6, 8, 1360) LCL _{NH} = 937 CL _{NH} = 1210			(8, 6, 1020) LCL _{NH} = 621 CL _{NH} = 876			(12, 4, 680) LCL _{NH} = 323 CL _{NH} = 545			(16, 3, 510) LCL _{NH} = 189 CL _{NH} = 384		
j	y_j	$\sum N_j$	j	y_j	$\sum N_j$	j	y_j	$\sum N_j$	j	y_j	$\sum N_j$	j	y_j	$\sum N_j$
1	1733	2040	1	1110	1360	1	792	1020	1	505	680	1	282	510
2	1981	4080	2	1209	2720	2	788	2040	2	504	1360	2	453	1020
3	2040	6120	3	1301	4080	3	1020	3060	3	501	2040	3	321	1530
4	2040	8160	4	1360	5440	4	749	4080	4	664	2720	4	278	2040
			5	1360	6800	5	1020	5100	5	653	3400	5	510	2550
			6	1163	8160	6	1020	6120	6	621	4080	6	339	3060
						7	1020	7140	7	680	4760	7	313	3570
						8	739	8160	8	615	5440	8	510	4080
									9	680	6120	9	437	4590
									10	680	6800	10	510	5100
									11	514	7480	11	453	5610
									12	483	8160	12	510	6120
												13	510	6630
												14	510	7140
												15	174	7650
												16	313	8160

7 Conclusions

In this paper, we have proposed an NBE-chart for monitoring the fraction nonconforming in FHP processes based on the negative hypergeometric distribution. This control chart addresses two crucial limitations of the commonly used binomial p -chart: it allows FHP processes and lot sizes to be monitored and it is quite efficient in monitoring processes with low fractions nonconforming. In the framework of an analytical comparison we have shown that the in-control interval of the negative hypergeometric NBE-chart is smaller than the in-control interval of the negative binomial NBE-chart when the process horizon is finite. That is, this chart is more sensitive to changes in the process fraction nonconforming, and relatively mild deteriorations of the process quality level can be detected in an effective way.

To appropriately consider the trade-off between on-target and out-of-target performance, we have proposed a conditional minimization procedure regarding the average number ANU of released units after the occurrence of the assignable cause, which allows the quality practitioner to know:

1. if the design of a desired sampling plan is operable,
2. what is the optimal sampling plan, and
3. what are respective out-of-target unit losses, defined as a penalty constant multiplying ANU.

Moreover, the performance study has confirmed that the negative hypergeometric NBE-chart is superior to its negative binomial counterpart and to the common binomial p chart especially for lower values of p in combination with lower values of N . These findings are in line with several simulations and numerical evidence given, e.g., in CHUKHROVA & JOHANNSEN^{44,45,51} and are caused by the fact that the binomial approximation to the hypergeometric considerably worsens for lower values of p and/or N .

Summarizing the results obtained in this paper, the investigated negative hypergeometric NBE-chart

1. is able to incorporate the process horizon by employing the negative hypergeometric distribution, that:

- accounts for the finite population effect on the probability of having nonconforming units within a lot (sampling without replacement scenario),
- does not assume the independence of successively sampled units,
- can not only be established for monitoring continuous processes (such as high-volume production) but also for monitoring FHP processes (such as batch and job/contract low-volume production),

2. is suitable for monitoring processes with low fractions nonconforming, and

3. is able to detect relatively mild deteriorations of the process quality level.

In addition, the negative hypergeometric NBE-chart is very flexible in implementing effects arising from varying lot size L , number of scheduled inspections m , inspection lot size N , and number of nonconforming unit(s) r (as often found in practice). Since the proposed negative hypergeometric NBE-chart is easy to implement in practical applications, it can directly be used to improve process monitoring in various fields, such as industrial quality control, service operations management, health care monitoring, public health surveillance, and in the pharmaceutical industry, where satisfaction of the above named requirements is of prior importance. Potential directions for promising future research are exemplary given by time weighted EWMA and/or CUSUM charts as well as a multivariate version of the proposed NBE-chart.

Acknowledgments:

The authors would like to thank for reviewer's valuable feedback and suggestions.

A Appendix

Proof of (3.2): Based on the general structure of a control chart with Shewhart-type control limits,

$$\text{UCL} = \mu + d_u\sigma \quad \text{CL} = \mu \quad \text{LCL} = \mu - d_l\sigma,$$

and by considering the random variable Y with $\mu = \mathbb{E}_{\text{NH}}[Y]$ and $\sigma = \sqrt{\text{Var}_{\text{NH}}(Y)}$, we get:

$$\begin{aligned} \text{UCL}_{\text{NH}} &= \mathbb{E}_{\text{NH}}[Y] + d_u\sqrt{\text{Var}_{\text{NH}}(Y)} \\ \text{CL}_{\text{NH}} &= \mathbb{E}_{\text{NH}}[Y] \\ \text{LCL}_{\text{NH}} &= \mathbb{E}_{\text{NH}}[Y] - d_l\sqrt{\text{Var}_{\text{NH}}(Y)} \end{aligned} \tag{A.1}$$

The variance term $\text{Var}_{\text{NH}}(Y)$ in (A.1) (given by (2.2)) can be simplified by using $N_1 = N+1$, $M_1 = M+1$, $\mathbb{E}_{\text{NH}}[Y] = rN_1(M_1)^{-1}$ as follows:

$$\begin{aligned} \text{Var}_{\text{NH}}(Y) &= \frac{rN_1(N_1 - M_1)(M_1 - r)}{(M_1)^2(M_1 + 1)} \\ &= \frac{rN_1(N_1 - rN_1(\mathbb{E}_{\text{NH}}[Y])^{-1})(rN_1(\mathbb{E}_{\text{NH}}[Y])^{-1} - r)}{(rN_1(\mathbb{E}_{\text{NH}}[Y])^{-1})^2(rN_1(\mathbb{E}_{\text{NH}}[Y])^{-1} + 1)} \\ &= \frac{(\mathbb{E}_{\text{NH}}[Y])^2(\mathbb{E}_{\text{NH}}[Y])^{-1}(\mathbb{E}_{\text{NH}}[Y] - r)(\mathbb{E}_{\text{NH}}[Y])^{-1}(rN_1 - \mathbb{E}_{\text{NH}}[Y])}{r(\mathbb{E}_{\text{NH}}[Y])^{-1}(rN_1 + \mathbb{E}_{\text{NH}}[Y])} \end{aligned}$$

$$= \mathbb{E}_{\text{NH}}[Y] \left(\frac{\mathbb{E}_{\text{NH}}[Y]}{r} - 1 \right) \frac{rN_1 - \mathbb{E}_{\text{NH}}[Y]}{rN_1 + \mathbb{E}_{\text{NH}}[Y]} \quad (\text{A.2})$$

Replacing $\mathbb{E}_{\text{NH}}[Y]$ in (A.1) and (A.2) by the target value Y_0 and substituting $\text{Var}_{\text{NH}}(Y)$ in (A.1) by (A.2) directly leads to (3.2). \square

References

- [1] XIE, M., T. N. GOH & G. P. RANJAN (2002): Some Effective Control Chart Procedures for Reliability Monitoring. *Reliability Engineering & System Safety*, **77**(2), pp. 143–150.
- [2] CHENG, Y., A. MUKHERJEE & M. XIE (2017): Simultaneously monitoring frequency and magnitude of events based on bivariate gamma distribution. *Journal of Statistical Computation and Simulation*, **87**(9), 1723–1741.
- [3] KUMAR, N., S. CHAKRABORTI & A. C. RAKITZIS (2017): Improved Shewhart-Type Charts for Monitoring Times Between Events. *Journal of Quality Technology*, **49**(3), pp. 278–296.
- [4] SANUSI, R. A. & A. MUKHERJEE (2019): A combination of max-type and distance based schemes for simultaneous monitoring of time between events and event magnitudes. *Quality and Reliability Engineering International*, **35**(1), 368–384.
- [5] ALEVIZAKOS, V. & C. KOUKOUVINOS (2020): A progressive mean control chart for monitoring time between events. *Quality and Reliability Engineering International*, **36**(1), pp. 161–186.
- [6] ALEVIZAKOS, V. & C. KOUKOUVINOS (2020): A double exponentially weighted moving average chart for time between events. *Communications in Statistics – Simulation and Computation*, **49**(10), pp. 2765–2784.
- [7] SANUSI, R. A., S. Y. TEH & M. B. KHOO (2020): Simultaneous monitoring of magnitude and time-between-events data with a Max-EWMA control chart. *Computers & Industrial Engineering*, **142**, 106378.
- [8] HU, X., P. CASTAGLIOLA, J. ZHONG, A. TANG & Y. QIAO (2021): On the performance of the adaptive EWMA chart for monitoring time between events. *Journal of Statistical Computation and Simulation*, **91**(6), pp. 1175–1211.
- [9] HU, X., Y. QIAO, P. ZHOU, J. ZHONG & S. WU (2021): Modified one-sided EWMA charts for monitoring time between events. *Communications in Statistics – Simulation and Computation*, in press.
- [10] ZHANG, C. W., M. XIE & T. N. GOH (2005): On Cumulative Conforming Type of Control Charts for High Quality Processes Under Sampling Inspection. *Economic Quality Control*, **20**(2), pp. 205–222.
- [11] ALI, S., A. PIEVATOLO & R. GÖB (2016): An Overview of Control Charts for High-quality Processes. *Quality and Reliability Engineering International*, **32**(7), pp. 2171–2189.
- [12] CALVIN, T. W. (1983): Quality Control Techniques for Zero-Defects. *IEEE Transactions on Components, Hybrids, and Manufacturing Technology*, **6**(3), pp. 323–328.
- [13] GOH, T. N. (1987): A Control Chart for very High Yield Processes. *Quality Assurance London*, **13**(1), pp. 18–22.
- [14] XIE, M. & T. N. GOH (1992): Some Procedures for Decision Making in Controlling High Yield Processes. *Quality and Reliability Engineering International*, **8**(4), pp. 355–360.
- [15] NELSON, L. S. (1994): A Control Chart for Parts-Per-Million Nonconforming Items. *Journal of Quality Technology*, **26**(3), pp. 239–240.
- [16] CHAN, L. Y., D. K. J. LIN, M. XIE & T. N. GOH (2002): Cumulative Probability Control Charts for

- Geometric and Exponential Process Characteristics. *International Journal of Production Research*, **40**(1), pp. 133–150.
- [17] KURALMANI, V., M. XIE & F. F. GAN (2002): A Conditional Decision Procedure for High Yield Processes. *IIE Transactions*, **34**(12), pp. 1021–1030.
- [18] RANJAN, P., M. XIE & T. N. GOH (2003): Optimal control limits for CCC charts in the presence of inspection errors. *Quality and Reliability Engineering International*, **19**(2), pp. 149–160.
- [19] ZHANG, L., K. GOVINDARAJU, M. BEBBINGTON & C. D. LAI (2004): On the Statistical Design of Geometric Control Charts. *Quality Technology & Quantitative Management*, **1**(2), pp. 233–243.
- [20] NOOROSSANA, R., A. SAGHAEI, K. PAYNABAR & Y. SAMIMI (2007): On the Conditional Decision Procedure for High Yield Processes. *Computers & Industrial Engineering*, **53**(3), pp. 469–477.
- [21] ACOSTA-MEJIA, C. A. (2012): Two-Sided Charts for Monitoring Nonconforming Parts per Million. *Quality Engineering*, **25**(1), pp. 34–45.
- [22] CHIU, J.-E. & C.-H. TSAI (2013): Properties and performance of one-sided cumulative count of conforming chart with parameter estimation in high-quality processes. *Journal of Applied Statistics*, **40**(11), pp. 2341–2353.
- [23] ZHANG, M., Y. PENG, A. SCHUH, F. M. MEGAHED & W. H. WOODALL (2013): Geometric charts with estimated control limits. *Quality and Reliability Engineering International*, **29**(2), pp. 209–223.
- [24] ZHANG, M., G. NIE & Z. HE (2014): Performance of cumulative count of conforming chart of variable sampling intervals with estimated control limits. *International Journal of Production Economics*, **150**, pp. 114–124.
- [25] GOLBAFIAN, V., M. S. FALLAHNEZHAD & Y. Z. MEHRJERDI (2017): A new Economic Scheme for CCC Charts with Run Rules based on average Number of inspected Items. *Communications in Statistics – Theory and Methods*, **46**(24), pp. 12023–12044.
- [26] MORAIS, M. C. (2017): ARL-unbiased Geometric and CCC_G Control Charts. *Sequential Analysis*, **36**(4), pp. 513–527.
- [27] OHTA, H., E. KUSAKAWA & A. RAHIM (2001): A $CCC-r$ Chart for High-Yield Processes. *Quality and Reliability Engineering International*, **17**(6), pp. 439–446.
- [28] CHAN, L. Y., C. D. LAI, M. XIE & T. N. GOH (2003): A Two-Stage Decision Procedure for Monitoring Processes with Low Fraction Nonconforming. *European Journal of Operational Research*, **150**(2), pp. 420–436.
- [29] DAS, N. (2003): Study on Implementing Control Charts Assuming Negative Binomial Distribution with Varying Sample Size in a Software Industry. *Software Quality Professional*, **6**(1), pp. 38–39.
- [30] DI BUCCHIANICO, A., G. D. MOOIWEER & E. J. D. MOONEN (2005): Monitoring Infrequent Failures of High-Volume Production Processes. *Quality and Reliability Engineering International*, **21**(5), pp. 521–528.
- [31] CHEN, J.-T. (2009): A new Approach to setting Control Limits of Cumulative Count of Conforming Charts for High-Yield Processes. *Quality and Reliability Engineering International*, **25**(8), pp. 973–986.
- [32] CHEN, J.-T. (2013): Design of Cumulative Count of Conforming Charts for High Yield Processes Based on Average Number of Items Inspected. *International Journal of Quality & Reliability Management*, **30**(9), pp. 942–957.
- [33] ALBERS, W. (2010): The optimal Choice of negative Binomial Charts for Monitoring High-Quality Processes. *Journal of Statistical Planning and Inference*, **140**(1), pp. 214–225.
- [34] ZHANG, M., X. HOU, H. CHEN & S. HE (2019): $CCC-r$ Charts' Performance with estimated Parameter for High-Quality Process. *Quality and Reliability Engineering International*, **35**(4), pp.

- 946–958.
- [35] CELANO, G. & P. CASTAGLIOLA (2018): The Shewhart F control chart for monitoring processes with finite number of inspections. *Quality and Reliability Engineering International*, **34**(8), pp. 1685–1698.
 - [36] NENES, G., P. CASTAGLIOLA, G. CELANO & S. PANAGIOTIDOU (2014): The variable sampling interval control chart for finite-horizon processes. *IIE Transactions*, **46**(10), pp. 1050–1065.
 - [37] NENES, G., P. CASTAGLIOLA & G. CELANO (2017): Economic and statistical design of V_p control charts for finite-horizon processes. *IIE Transactions*, **49**(1), pp. 110–125.
 - [38] CELANO, G., P. CASTAGLIOLA, S. CHAKRABORTI & G. NENES (2015): The performance of the Shewhart sign control chart for finite horizon processes. *The International Journal of Advanced Manufacturing Technology*, **84**, pp. 1497–1512.
 - [39] CELANO, G., P. CASTAGLIOLA, S. CHAKRABORTI & G. NENES (2016): On the implementation of the Shewhart sign control chart for low-volume production. *International Journal of Production Research*, **54**(19), pp. 5886–5900.
 - [40] CELANO, G. & P. CASTAGLIOLA (2018): An EWMA sign control chart with varying control limits for finite horizon processes. *Quality and Reliability Engineering International*, **34**(8), pp. 1717–1731.
 - [41] CELANO, G., P. CASTAGLIOLA & S. CHAKRABORTI (2016): Joint Shewhart control charts for location and scale monitoring in finite horizon processes. *Computers & Industrial Engineering*, **101**(19), pp. 427–439.
 - [42] CELANO, G. & P. CASTAGLIOLA (2020): On-line monitoring of extreme values of geometric profiles in finite horizon processes. *Quality and Reliability Engineering International*, **36**(4), pp. 1313–1332.
 - [43] CELANO, G. & S. CHAKRABORTI (2021): A distribution-free Shewhart-type Mann–Whitney control chart for monitoring finite horizon productions. *International Journal of Production Research*, **59**(20), pp. 6069–6086.
 - [44] CHUKHROVA, N. & A. JOHANNSEN (2019): Improved control charts for fraction non-conforming based on hypergeometric distribution. *Computers & Industrial Engineering*, **128**, pp. 795–806.
 - [45] CHUKHROVA, N. & A. JOHANNSEN (2019): Hypergeometric p -chart with dynamic probability control limits for monitoring processes with variable sample and population sizes. *Computers & Industrial Engineering*, **136**, pp. 681–701.
 - [46] JOHANNSEN, A., N. CHUKHROVA & P. CASTAGLIOLA (2022): The performance of the hypergeometric np chart with estimated parameter. *European Journal of Operational Research*, **296**(3), pp. 873–899.
 - [47] BENNEYAN, J. C. (2001): Number-Between g -Type Statistical Quality Control Charts for Monitoring Adverse Events. *Health Care Management Science*, **4**(4), pp. 305–318.
 - [48] JOHNSON, N. L., A. W. KEMP & S. KOTZ (2005): *Univariate Discrete Distributions*. 3rd edition, John Wiley & Sons, Inc.
 - [49] PANAGIOTIDOU, S. & G. TAGARAS (2010): Statistical process control and condition-based maintenance: A meaningful relationship through data sharing. *Production and Operations Management*, **19**(2), pp. 156–171.
 - [50] BENNEYAN, J. C. (2001): Performance of Number-Between g -Type Statistical Control Charts for Monitoring Adverse Events. *Health Care Management Science*, **4**(4), pp. 319–336.
 - [51] CHUKHROVA, N. & A. JOHANNSEN (2019): Improved Binomial and Poisson Approximations to the Type-A Operating Characteristic Function. *International Journal of Quality & Reliability Management*, **36**(4), pp. 620–652.